Zero Emissions Research and Technology (ZERT) II – Investigating the Fundamental Scientific Issues Affecting the Long-term Geologic Storage of Carbon Dioxide

Project Number DE-FE0000397

Lee H Spangler

Energy Research Institute

Montana State University

•U.S. Department of Energy

•National Energy Technology Laboratory

•Carbon Storage R&D Project Review Meeting

•Developing the Technologies and

•Infrastructure for CCS

•August 12-14, 2014

Presentation Outline

- Laboratory studies to understand subsurface CO_2 behavior
- Mitigation method development bio-sealing of shales
- Fiber sensor development
  – Soil CO_2 sensor
  – Distributed borehole seismic sensor
- Coal bed methane enhancement / mitigation
- Analog studies to inform risk analysis

Benefit to the Program

Program goals being addressed.

- Develop technologies that will support industries' ability to predict CO_2 storage capacity in geologic formations to within ±30 percent.
- Develop technologies to demonstrate that 99 percent of injected CO_2 remains in the injection zones.
- Conduct field tests through 2030 to support the development of BPMs for site selection, characterization, site operations, and closure practices.

Project benefits statement.

ZERT II supports Storage Program goals by 1) developing computational tools for simulating CO_2 injection, storage and trapping, 2) performing basic geoscience experiments to address relationships between properties such as wetting, relative permeability, saturation, and capillary pressure that will improve understanding of CO_2 behavior in the reservoir and help with model parameterization 3) investigating analogs to understand risks to storage security 4) conducting field experiments to test near surface monitoring technologies and 5) developing novel bio-controlled leakage mitigation technology

Project Overview:
Goals and Objectives

Fundamental Geosciences

- Objective: Develop methods to perform *in situ* measurements during core flood and flow experiments

Biofilms, Biomineralization and Biogenic Processes

- Objective: Perform a comprehensive evaluation of techniques for current and novel CO_2 sequestration concepts associated with microbial biofilms.
- Objective: Evaluate the potential for coal-bed mediated CO2 sequestration and enhanced methane production.

Natural Analogs of Escape Mechanisms

- Objective: Characterize the physical, mineralogical, and geochemical characteristics of outcrops of hydrothermal plume related rocks to determine their usefulness as natural analogs of breached and healed caprocks for carbon sequestration.

Optical Detection for Carbon Sequestration Site Monitoring

- Objective: Demonstrate the feasibility of creating an in-line fiber optic sensor for CO_2 that utilizes sections of photonic bandgap (PBG) fibers interspersed with sections of single mode optical fiber.
- Objective: Develop a low cost multispectral imager to detect CO_2 -induced plant stress

Validation of Near-surface CO_2 Detection Techniques and Transport Models

- Objective: Determine, via field experimentation, the efficacy and detection limits for existing and emerging near-surface CO_2 detection technologies.

Technical Status

- Focus the remaining slides, logically walking through the project. Tell the story of your project and highlight the key points as described in the Presentation Guidelines. Organize the remainder of the talk as though it was being given at a technical conference.
- When providing graphs or a table of results from testing or systems analyses, also indicate the baseline or targets that need to be met in order to achieve the project and program goals.

Capabilities for *in-situ* MRI studies of CO_2/brine in rock cores at Montana State University

Sarah L. Codd, Joseph D. Seymour, Joshua M. Bray, and Cody A. Prather

Magnetic Resonance Microscopy (MRM) lab

June 22, 2014

Temco custom FCH Core Holder

Core Holder Schematic

A. Core-challenge fluid (outlet)
B. Recirculating fluid (outlet)
C. Recirculating fluid (inlet)
D. Core-challenge fluid (inlet)
E. Thermocouple
F. PEEK composite sheath

Max. pressure: 5000 psi
Max. temperature: 150°C

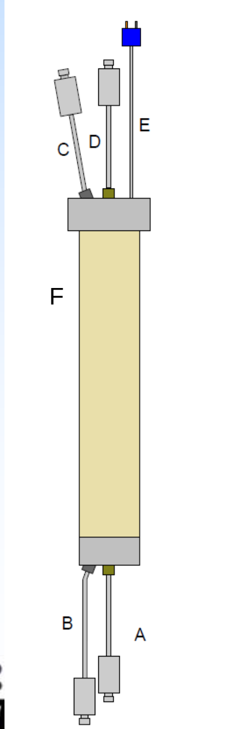

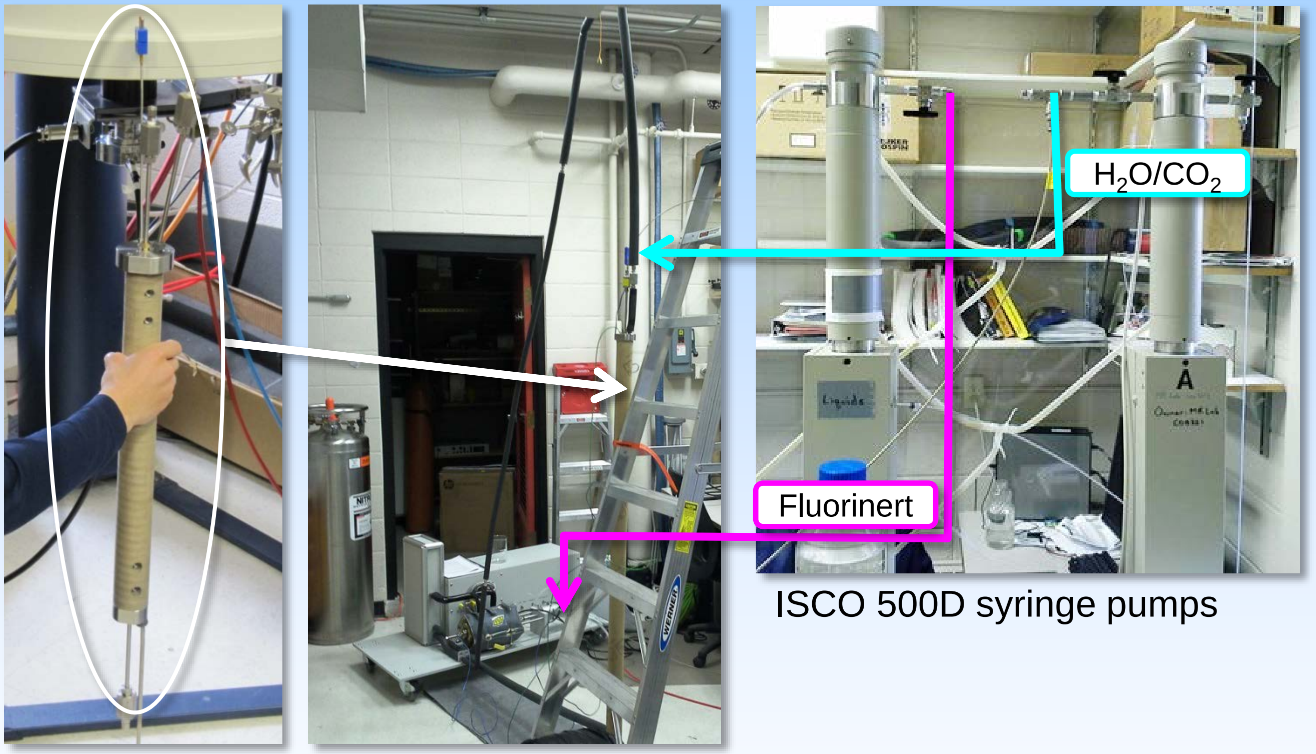

Core holder

Flow loop mock-up

ISCO 500D syringe pumps

Previous strategy: 3D spin-echo imaging

Limestone Sandstone

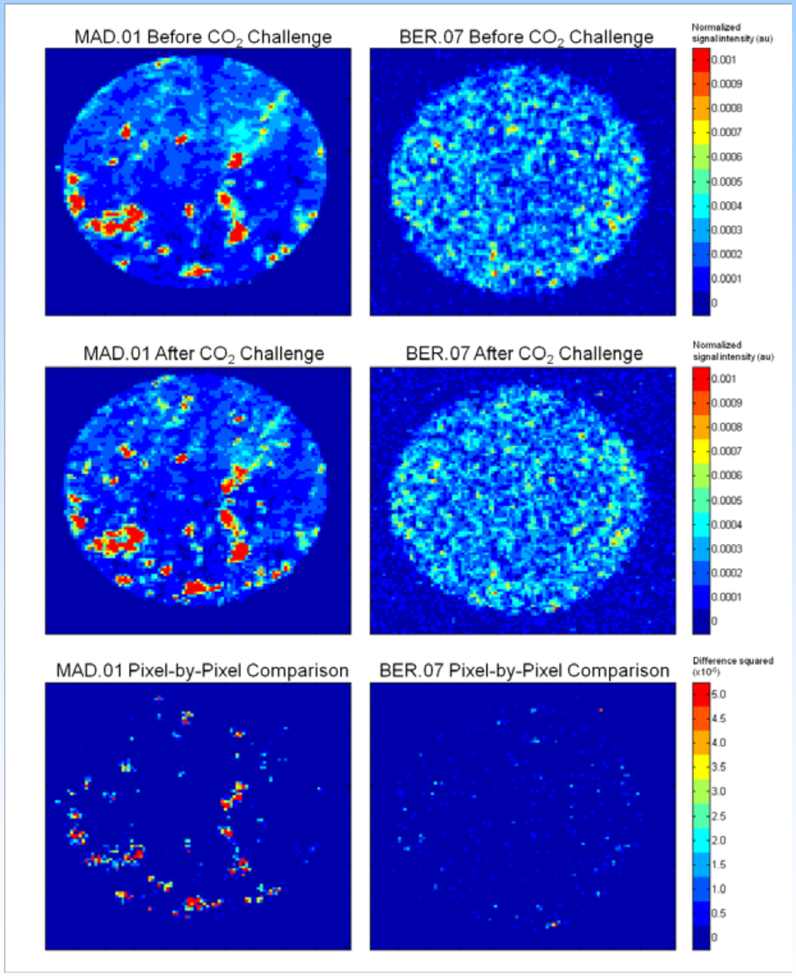

Limestone

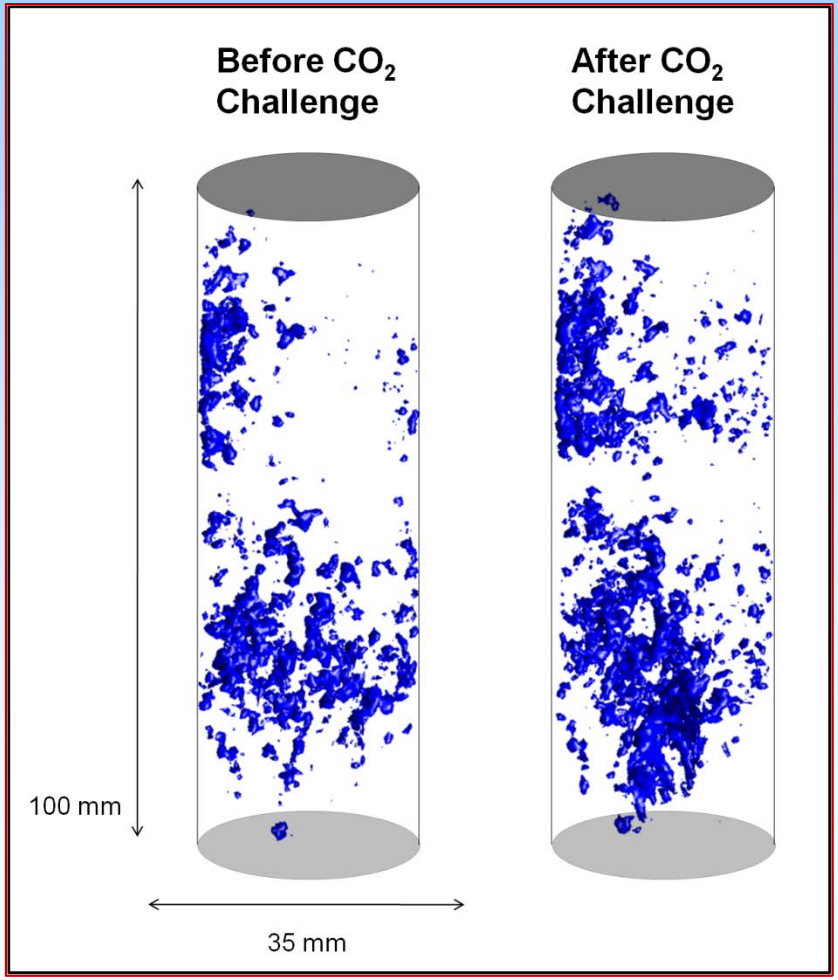

C. A. Shaw, S. J. Vogt, J. E. Maneval, T. Brox, M. L. Skidmore, S. L. Codd, J. D. Seymour, "Physical and Chemical Effects of Two-Phase Brine/Supercritical-CO2 Fluid Flow on Clastic Rocks: Real-Time Monitoring and NMR Imaging of Flow-Through Core Experiments", Poster: GC31C-0896, Fall Meeting, AGU, San Francisco, Calif., Dec. 13-17, 2010

MRI Sequence Comparison

<u>Spin-echo imaging (SEI)</u>

- **High resolution**
- **Slower**, repetition-time-limited acquisition
- **High power** demands
- Gradient **noise/vibration**

<u>Zero echo time imaging (ZTE)</u>

- Bandwidth limited (**lower resolution**)
- **Rapid**, steady-state k-space acquisition
- **Low power** demands
- "Silent mode", **low vibration**

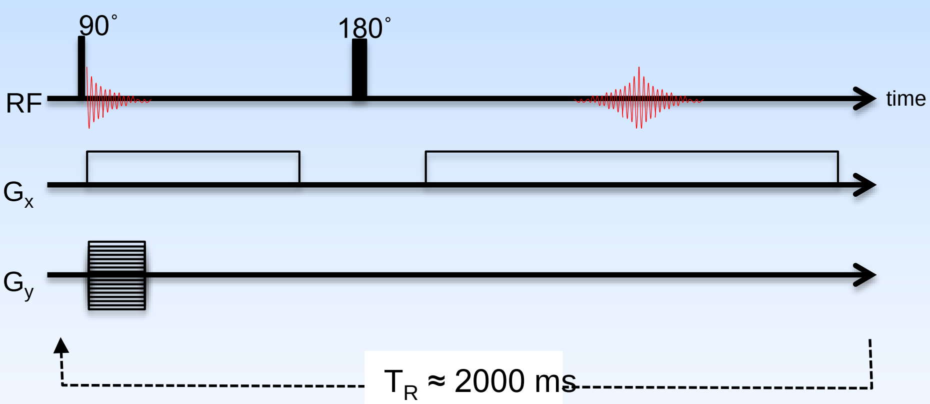

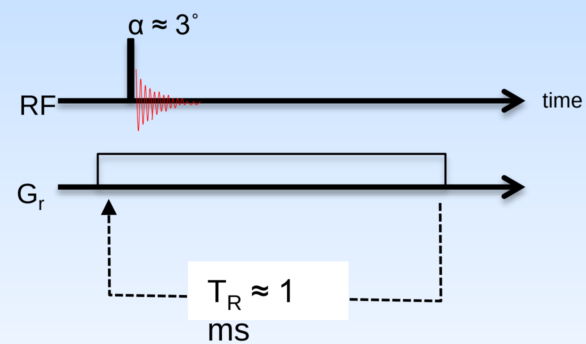

	<u>SEI</u>	<u>ZTE</u>
Total scan time:	30 hours	**53 sec.**
Image resolution:	270 × 270 × 1500 µm	(781 µm)^3

Zero Emissions Research and Technology

MONTANA STATE UNIVERSITY

ZTE imaging demonstration:
H_2O displacement by injected CO_2 gas in Berea core

1. Initially dry core

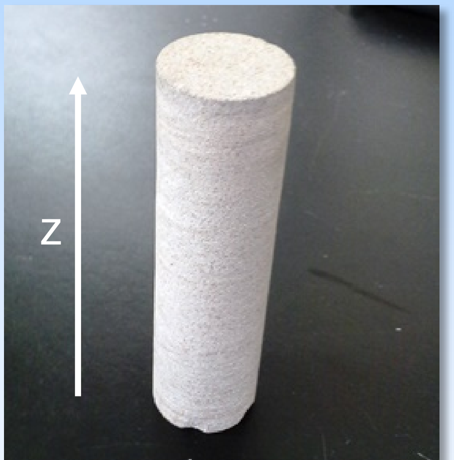

2. Mount in core holder/RF coil

3. Acquire 3D images with ZTE

4. Water distribution in 1D
a) Dry core
b) Inject H_2O (full saturation)
c) Inject CO_2 (H_2O displacement)

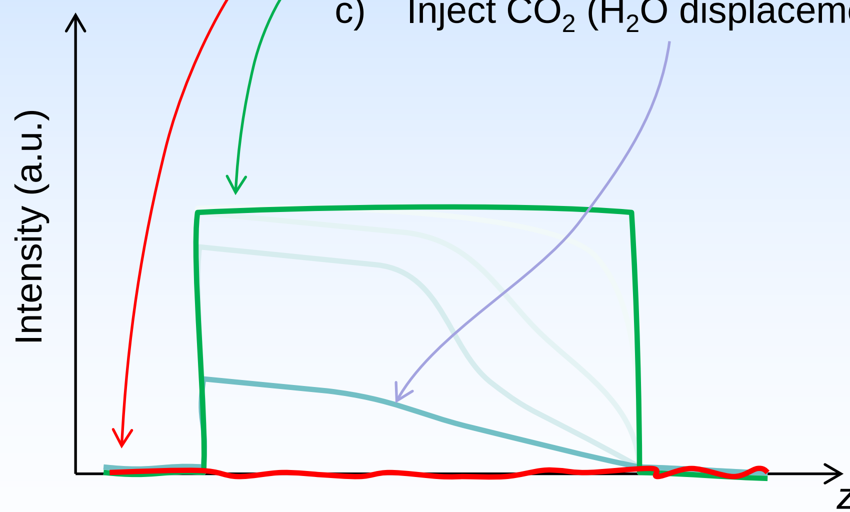

Rock core images – Background signal subtraction

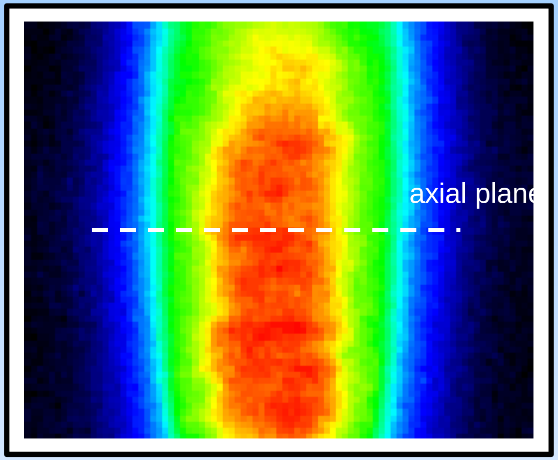

Rock core, MRI side-view

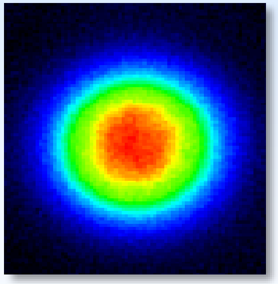 - 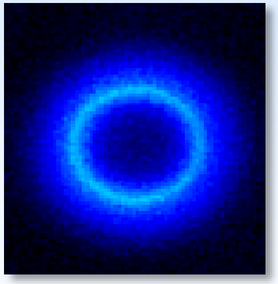 = 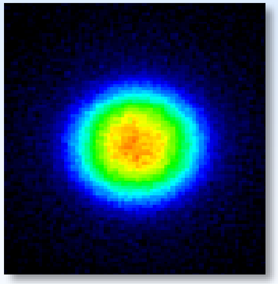

Image of saturated core | Image with dry core | Saturated core *<u>only</u>*

Sources of ^{1}H background signal:

- **Plastics of the RF coi**l
  currently having them retrofitted!
- **AFLAS overburden sleeve**
  have a FEP heat-shrink sleeve with no signal

Rock core images – CO_2 injection test

- 1 sagittal plane (lengthwise); 3 axial planes: top, middle, bottom
- FOV: 100 × 100 × 100 mm^3
- Resolution: 781 µm
- Time step: 3 min. 30 sec. (53 second scan time)

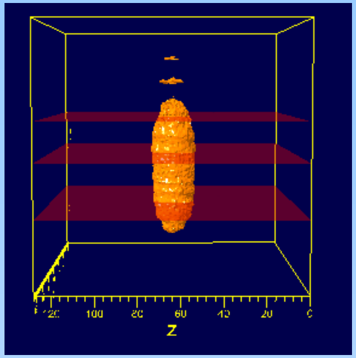

Fully-saturated core

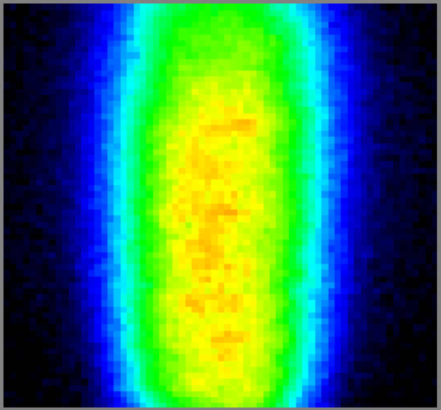

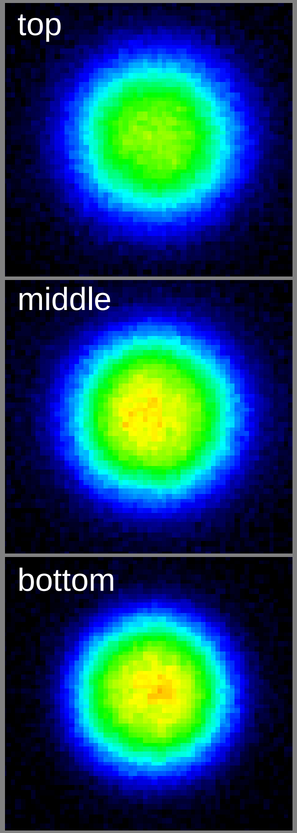

CO_2 pulse in transit

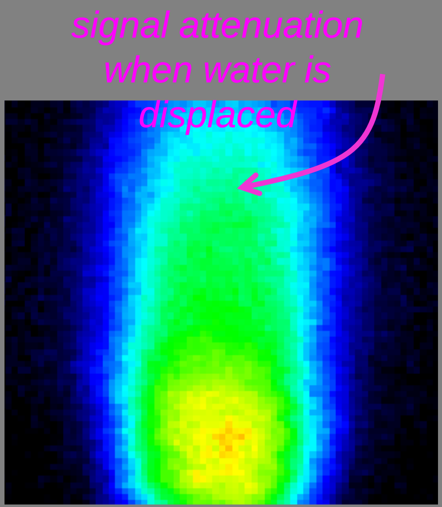

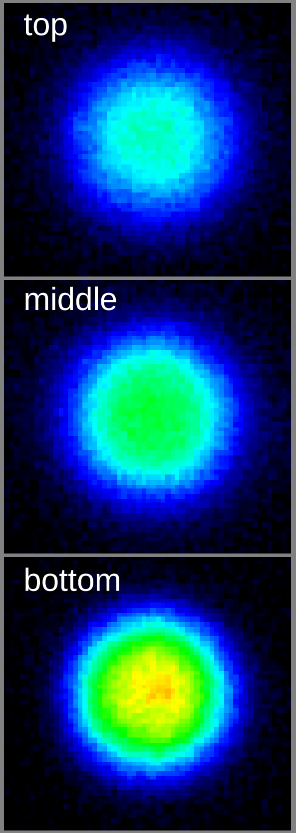

MONTANA STATE UNIVERSITY

Rock core images – CO_2 injection test

- 1-D projection of signal intensity
- Time step is 3 min. 30 sec.

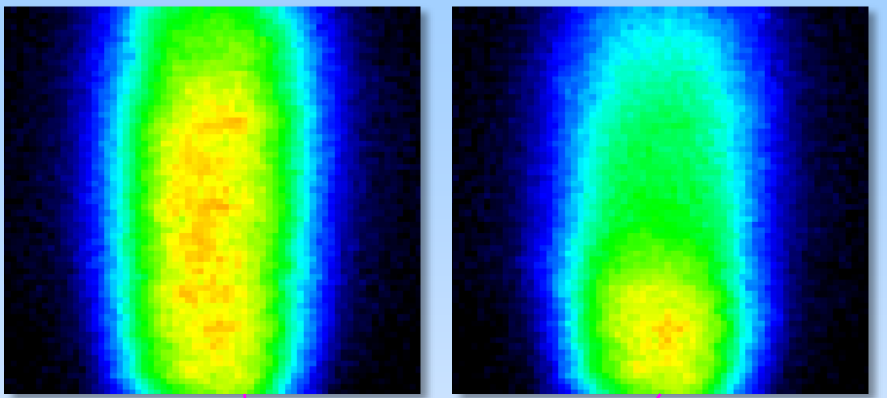

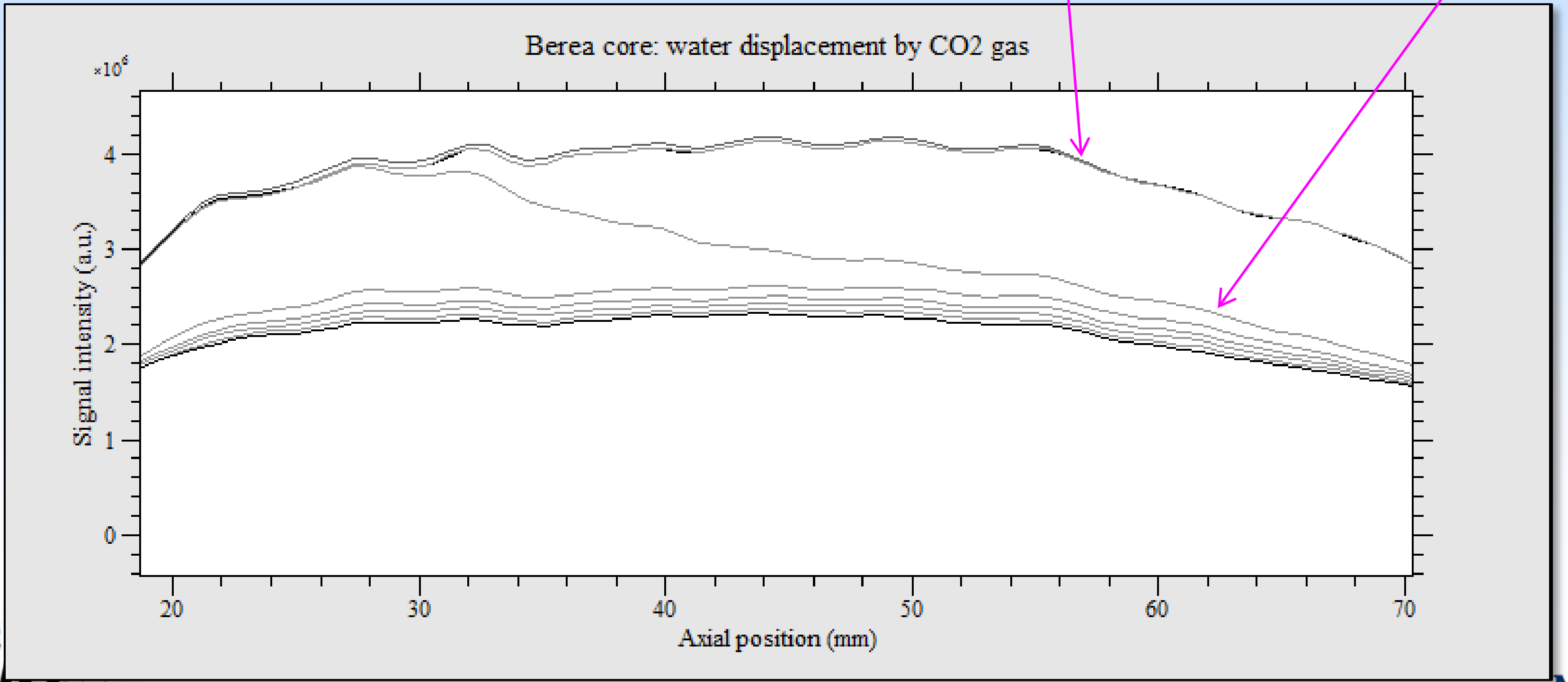

Acidic solutions

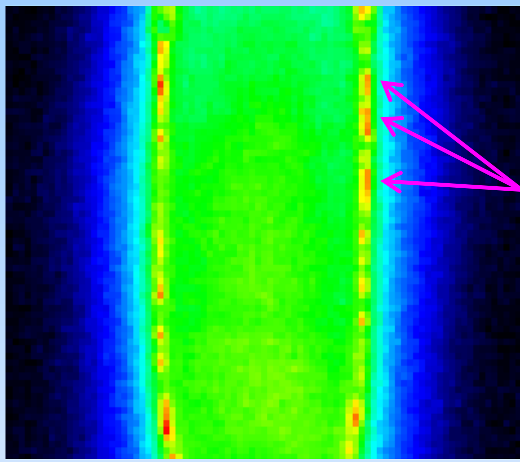

Bright spots in the overburden sleeve?...

Late-time point

Acid damage in the headspace!

Align distribution plugs to avoid dead volume.

Temco is sending replacements free of charge.

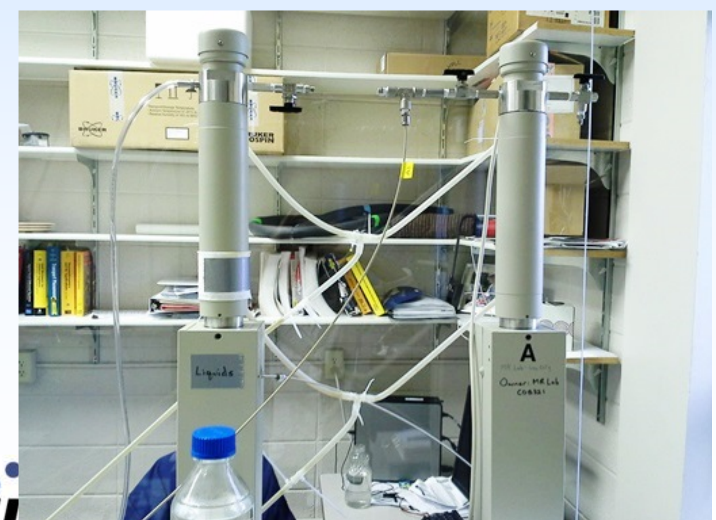

Switching between liquid/CO_2 in pump

Extra ISCO 500D pump

Potential for long-duration studies

Capabilities summary

The Temco MRI-compatible core holder enables us to:

1. Observe water in real, porous rock cores
2. Inject liquids, gases, or supercritical fluids (brine, CO_2, etc.)
3. Acquire 3D images in 50 sec. with ~1 mm resolution
4. Observe transport and structural changes *in situ*

Microbially Induced Carbonate Precipitation (MICP)

Cunningham, Gerlach

+ pH and alkalinity (increase in OH^- and HCO_3^-) increase SATURATION STATE OF CALCITE

$$CO(NH_2)_2 + H_2O \rightarrow NH_2COOH + NH_3$$
$$\underline{NH_2COOH + H_2O \rightarrow NH_3 + H_2CO_3}$$
$$CO(NH_2)_2 + 2\ H_2O \rightarrow 2\ NH_3 + H_2CO_3$$ (Urea hydrolysis)

$$2NH_3 + 2H_2O \leftrightarrow 2NH_4^+ + \boxed{2OH^-}$$ (pH increase)

$$H_2CO_3 + 2OH^- \leftrightarrow HCO_3^- + H_2O + OH^- \leftrightarrow \boxed{CO_3^{2-}} + 2\ H_2O$$

$$CO_3^{2-} + Ca^{2+} \leftrightarrow \boxed{CaCO_3}$$ (carbonate precipitation)

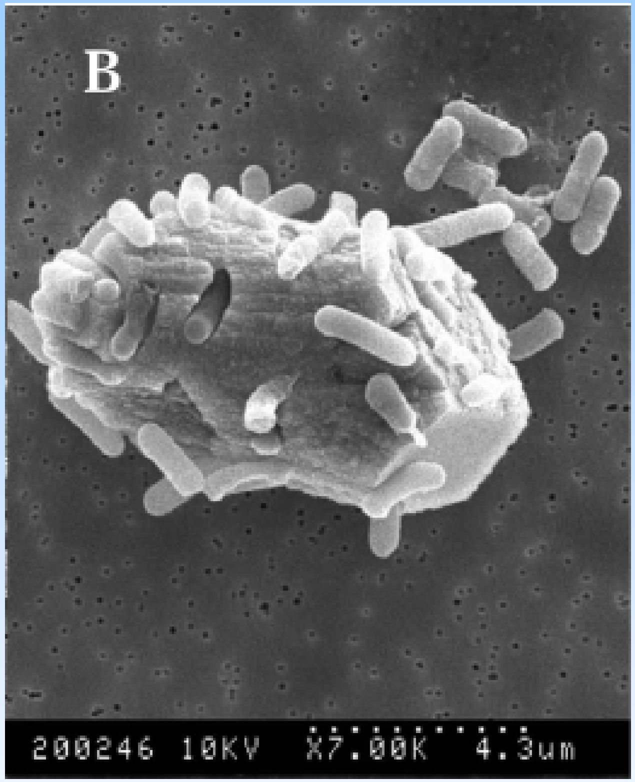

Model ureolytic organism: *Sporosarcina pasteurii*

Ureolysis is only one possible way to manipulate the saturation state of carbonates

Mitchell, AC and Ferris, FG (2006). *Geomicrobiology Journal* , 23, 213-226.

Mitchell, AC. and Ferris, FG. (2006) *Environmental Science and Technology, 40, 1008-1014.*

Mitchell, AC. and Ferris FG. (2005) *Geochimica Et Cosmochimica Acta, 69, 4199-4210.*

Bio-sealants in Mont Terri
Conducted by Montana State University

Permeability reduction due to biomineralization in one-inch diameter Opalinus shale core drilled from original shale sample, July 18, 2013

Core locations on the Opalinus shale sample

ZERT Zero Emissions Research and Technology

MONTANA STATE UNIVERSITY

X-Ray CT scans for two locations along the axis of core OP1-4

Slice 1

Slice 2

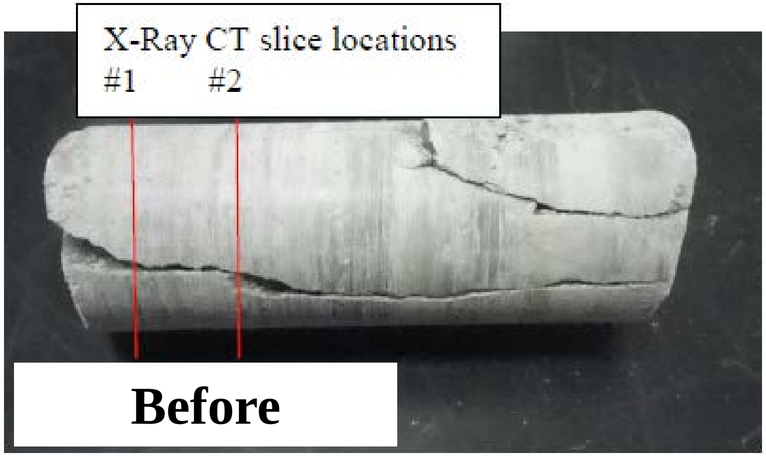

a)

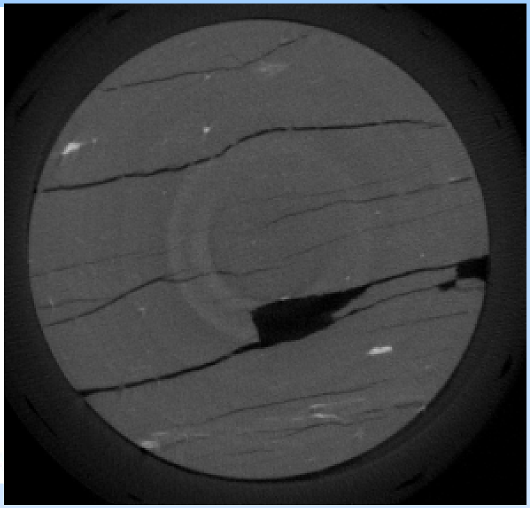

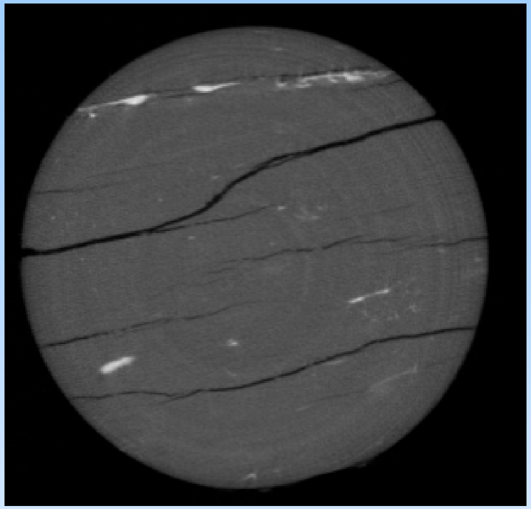

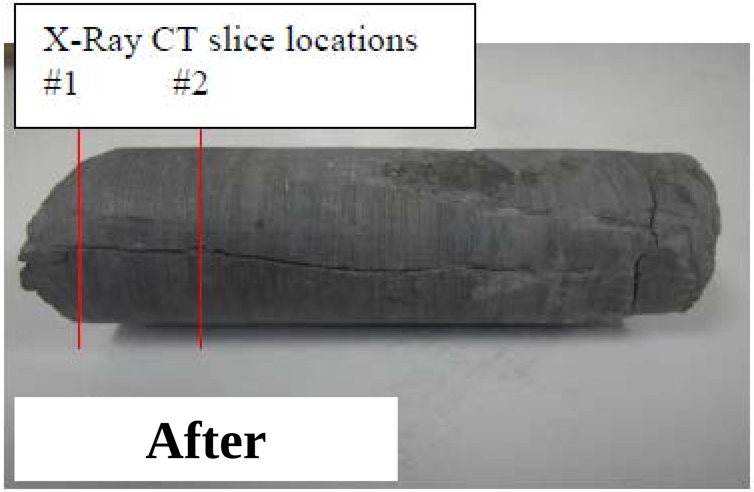

b)

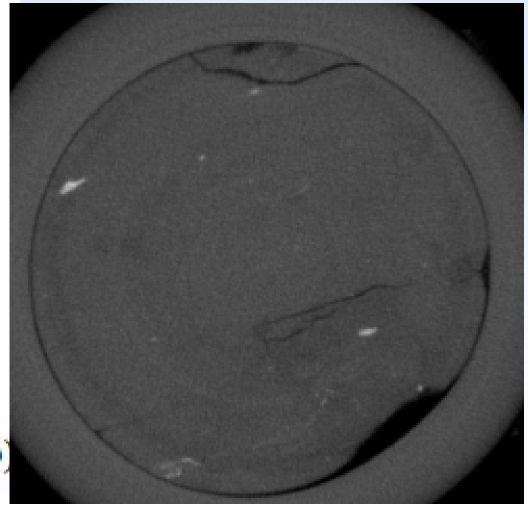

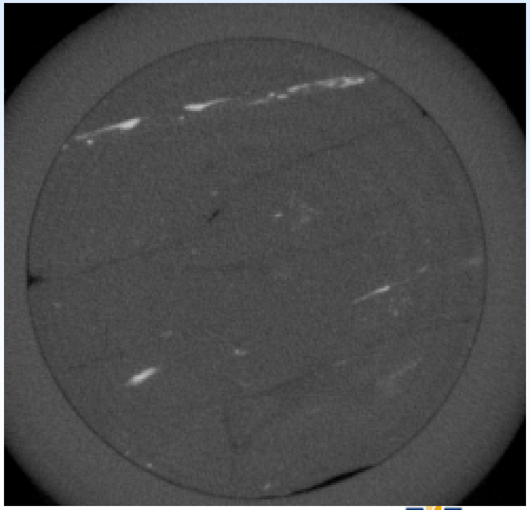

ZERT Zero Emissions Research and Technology

MONTANA STATE UNIVERSITY

Permeability Tests With & Without Propants

Split OP2-3 core and core wrapped in PTFE tape. Core length was 5.77 cm

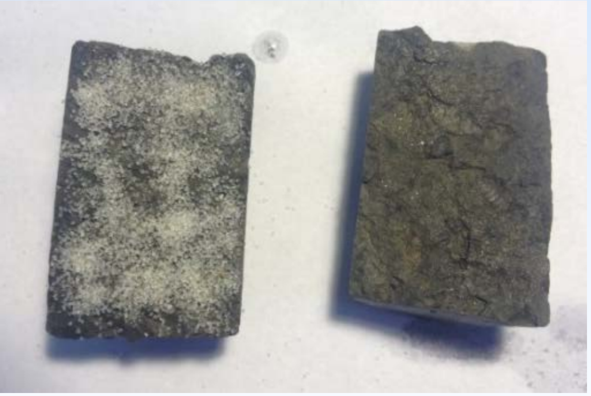

OP2-4 Core showing proppant placement and wrapping pieces with PTFE tape

Table 1 Initial Permeability values prior to biomineralization					
Core	Area (cm^2)	Average Length (cm)	Flow Rate (ml/min)	Pressure drop (meters H_2O)	Calculated Permeability (mD)
OP2-3	5.43	5.77	10.0	7.3	249
OP2-4	5.43	4.01	40.0	2.2	2,420

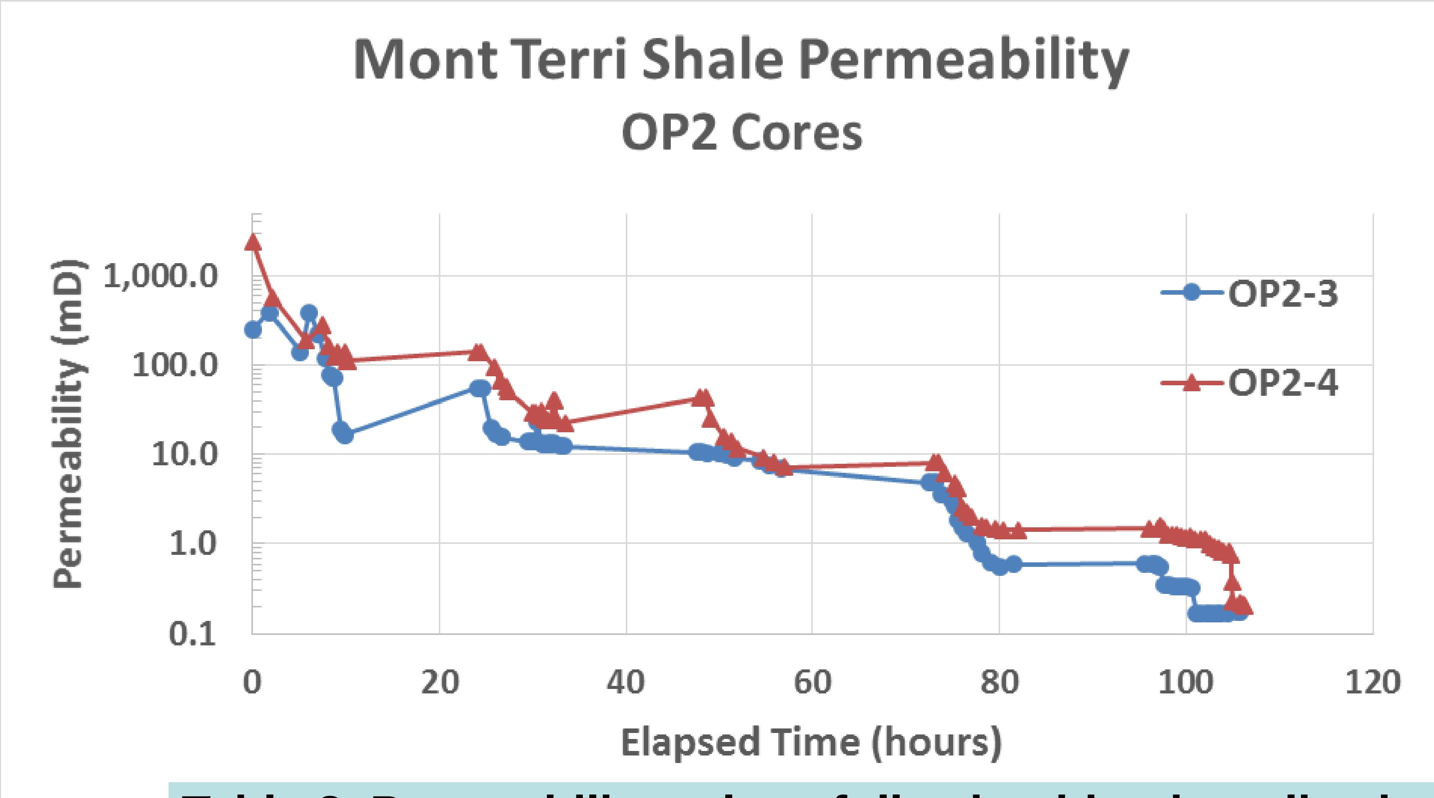

Table 2 Permeability values following biomineralization				
Core	Flow Rate (ml/min)	Pressure drop (meters H_2O)	Final Permeability (mD)	Permeability Reduction
OP2-3	0.015	15.6	0.18	99.93%
OP2-4	0.03	19.5	0.20	99.99%

Inline Fiber Sensor

K. Repasky

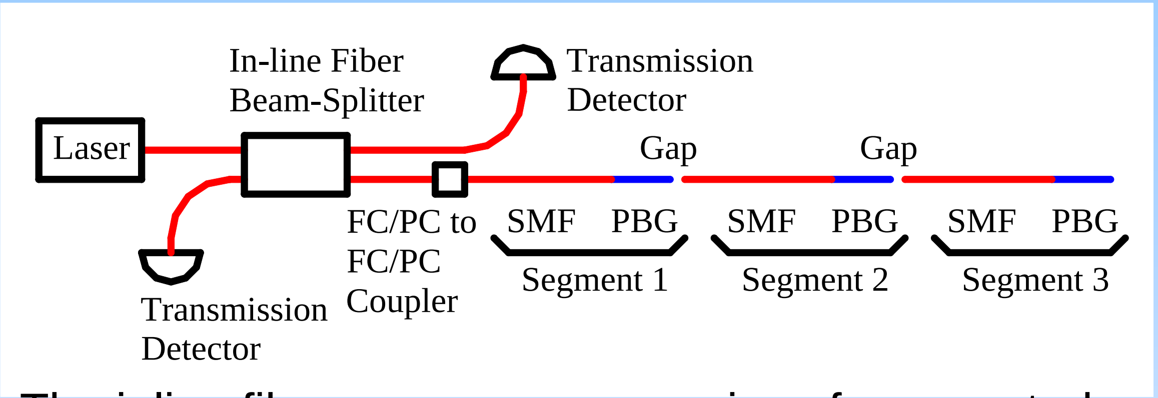

The inline fiber sensor uses a series of segmented photonic bandgap (PBG) fiber in series to for a inline fiber sensor array.

Each segment is addressed using time of flight of the laser pulse.

CO_2 diffuses into the PBG fiber to allow spectroscopic measurements of CO_2 concentration.

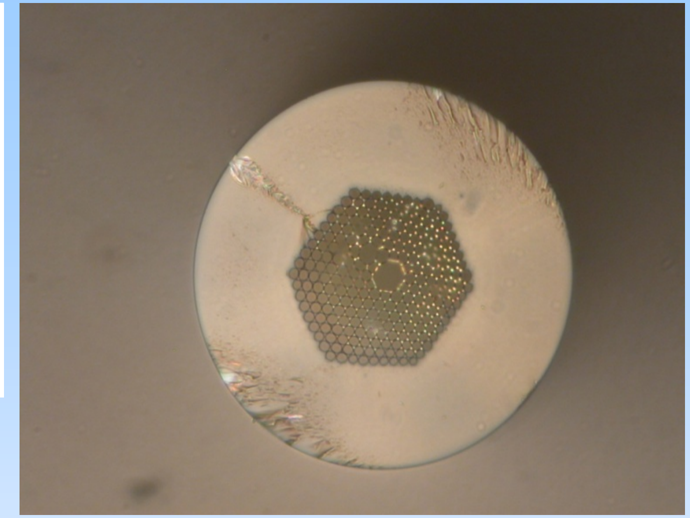

The PBG fiber allows interaction of the laser light and CO_2 in the hollow core.

Challenge: PBG fiber is larger diameter than SMF and conventional splicing collapses hollow core

ZERT Zero Emissions Research and Technology

MONTANA STATE UNIVERSITY

Fiber Sensors

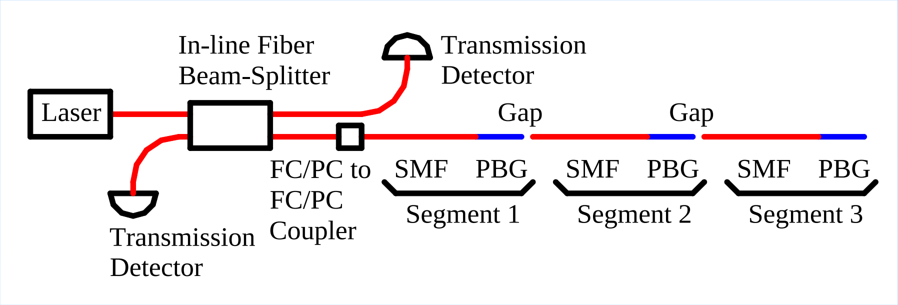

Schematic of the inline fiber sensor. Carbon dioxide measurements can be made in each of the photonic bandgap (PBG) fibers.

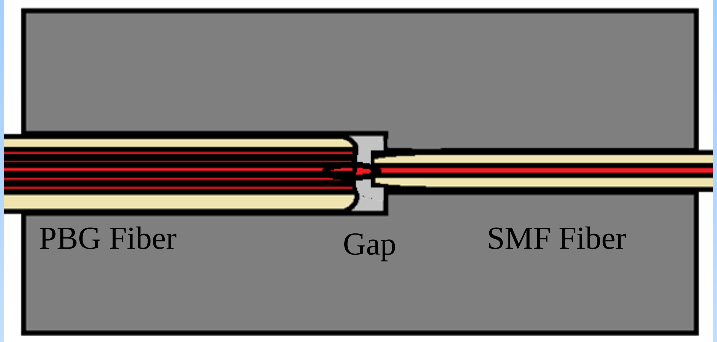

After each PBG fiber section, a gap allows a portion of the light to be reflected back to the detector while the remainder of the light couples into a SMF fiber. The gap spacing determines the reflectivity.

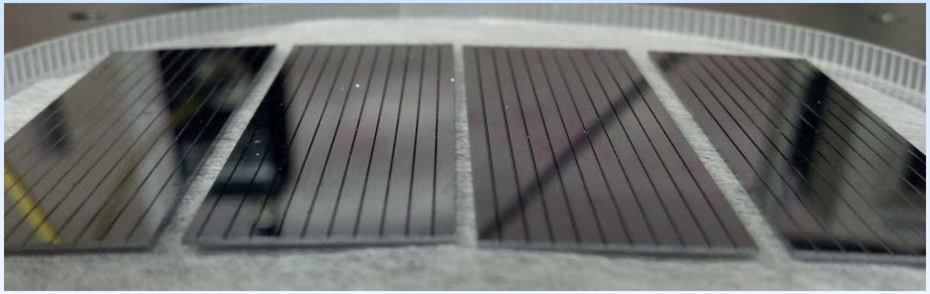

V-groove structures where designed and manufactured allowing precise and repeatable alignment of the PBG fiber and SMF fiber.

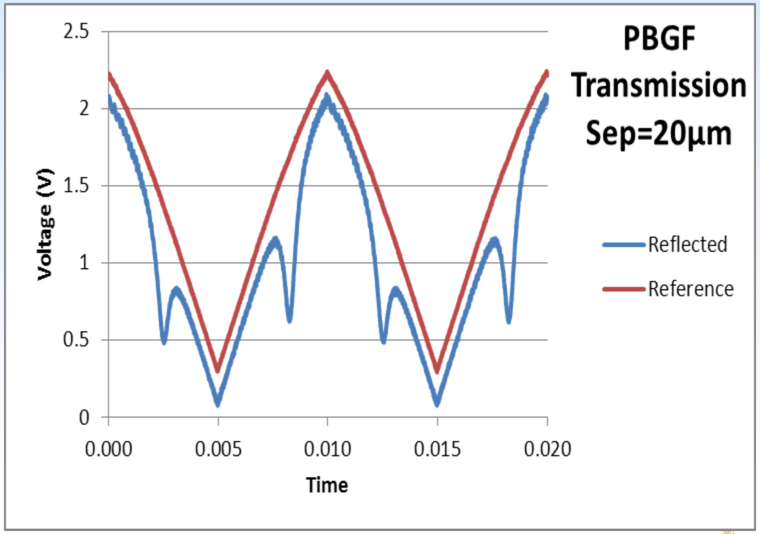

The transmitted light during a wavelength scan is shown as the red line. The light reflected from the second segment of the inline fiber sensor is shown as the blue line. Dividing these two signal would yield a transmission spectrum. The carbon dioxide absorption feature is seen in the reflected signal and can be used to monitor carbon dioxide concentrations.

ZERT Zero Emissions Research and Technology

MONTANA STATE UNIVERSITY

Fiber Sensors

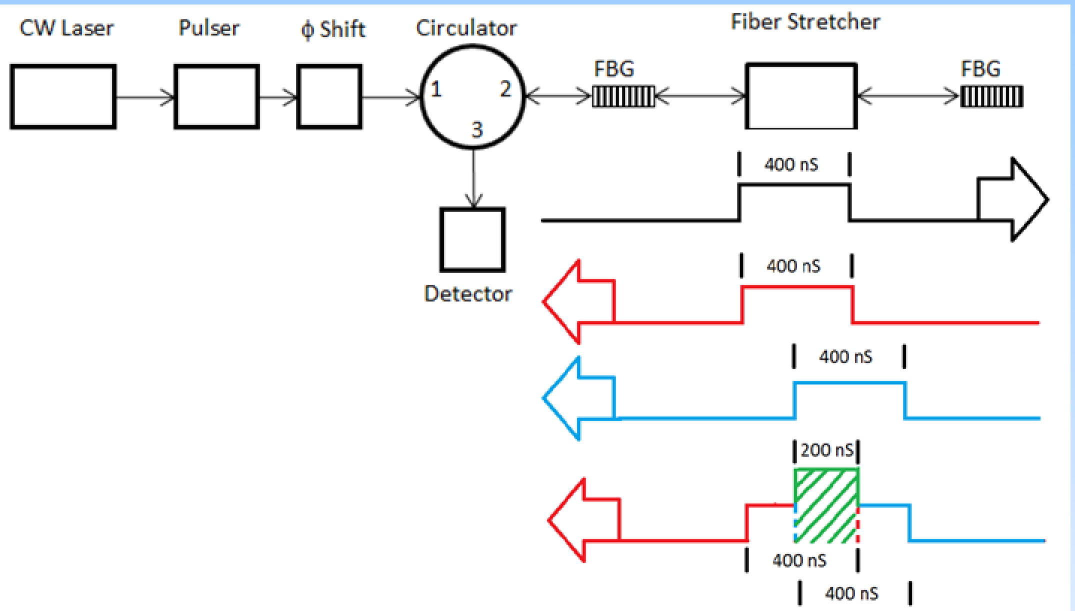

A single section of the distributed fiber seismic sensing system schematic, the 400ns pulse is sent down the FGB line, the fiber stretcher will alter the path length between the two FBG's which will change the amplitude of the 200ns interference signal created by the two overlapping reflected 400ns pulses. A fiber stretcher was used to mimic the effects of a seismic wave.

The fiber seismic sensor set up for laboratory testing. The ability to measure seismic events over a distributed fiber seismic sensor array has the potential to allow monitoring of the injected carbon dioxide plum.

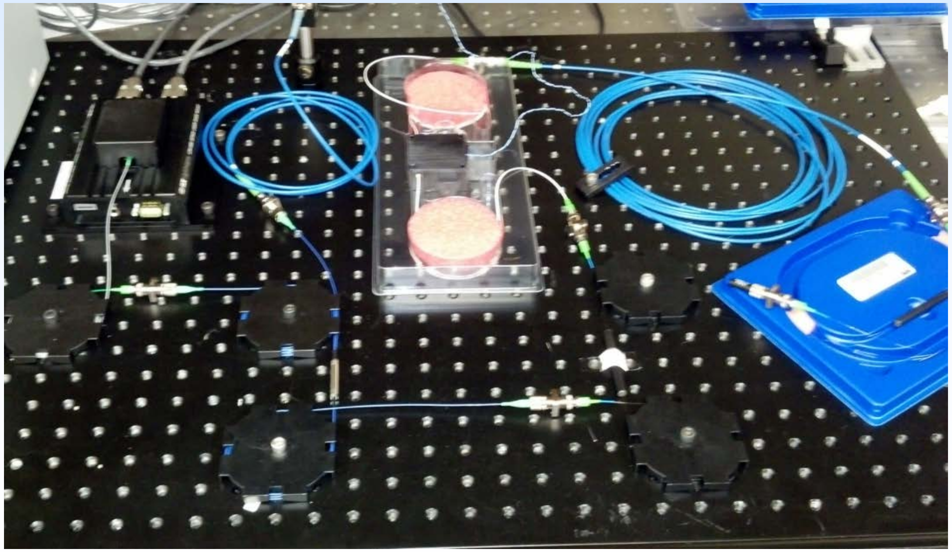

ZERT Zero Emissions Research and Technology

MONTANA STATE UNIVERSITY

Fiber Sensors

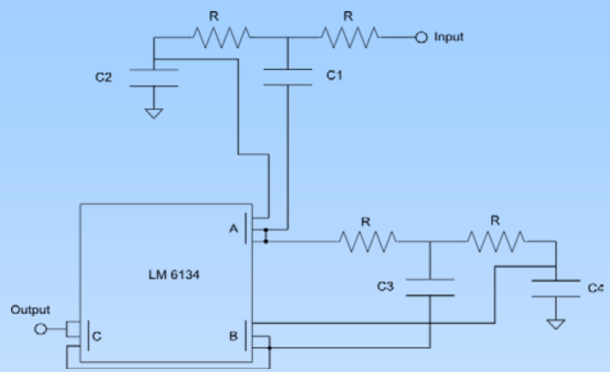

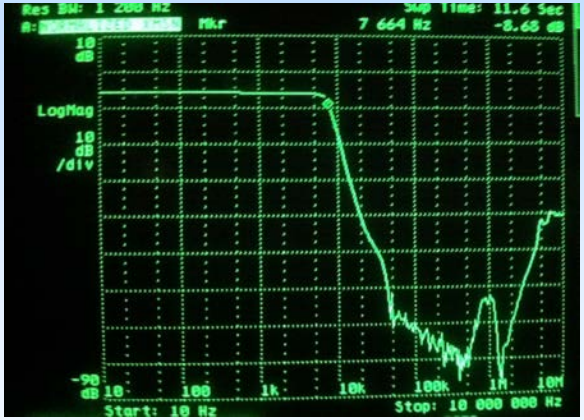

Careful filtering of the signal is needed to achieve good signal to noise performance. An active filter was designed as shown in the upper schematic with the Bode plot showing the filter frequency response in the lower plot. The corner frequency can be changed while maintaining the 60 dB/decade falloff.

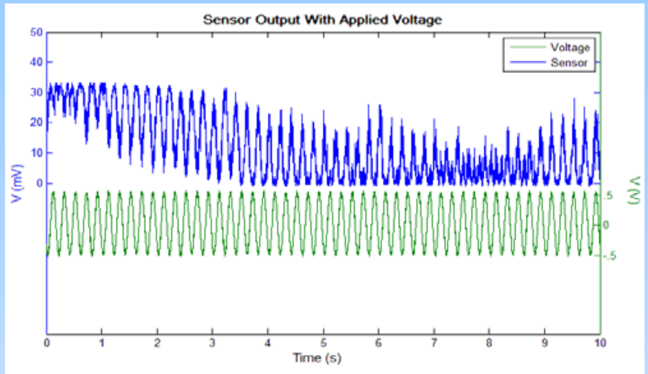

The bottom (green) line represents the signal sent to the fiber stretcher while the top (blue) line represents the signal seen by the fiber sensor.

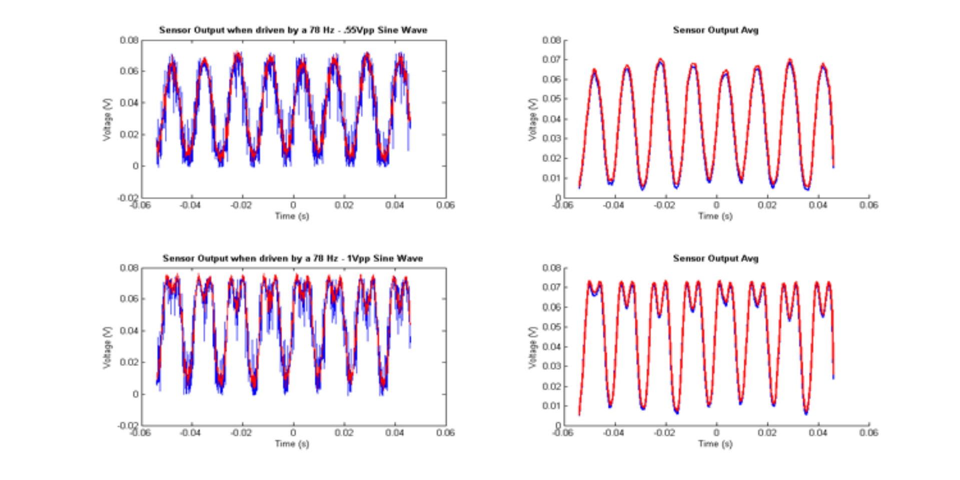

Fiber sensor signal as a function of time. The blue line for the plots on the left represent the unfiltered signal while the red line represents the filtered signal. The right hand plots utilizes a sliding window averaging. The strain sensitivity of the fiber sensor is measured to be 60×10^{-9} indicating this sensor can work for subsurface seismic monitoring.

MONTANA STATE UNIVERSITY
Fields, Cunningham

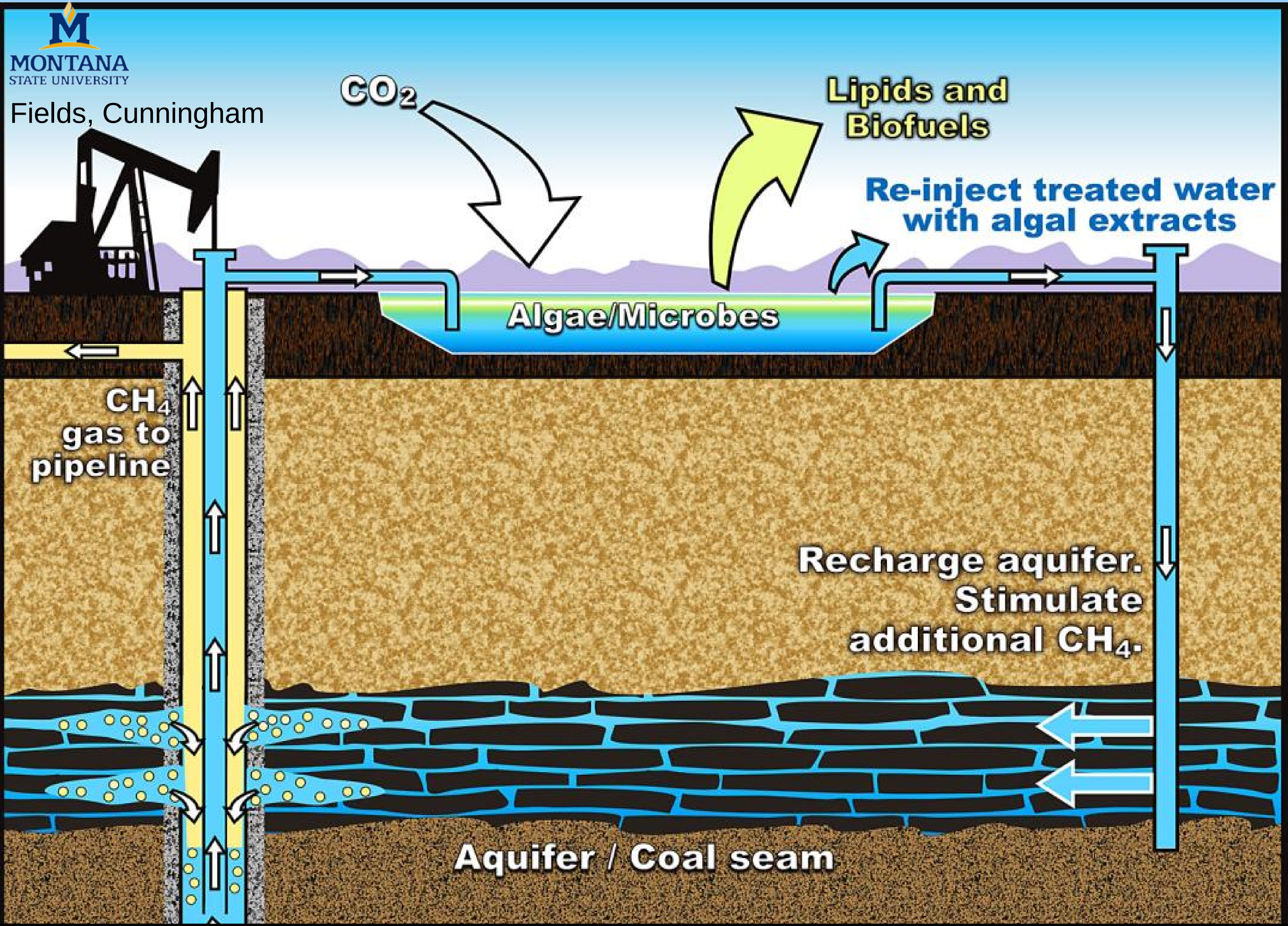

Algae enhanced CBM Microcosm experiments

Three sets of microcosm experiments have been run and are continuing at present. These microcosm experiments all involve the addition of algae extract as a stimulant to methane production from coal, compared to methane production from the same coal without algae addition. The description of each experiment is as follows.

Experiment 1. Coal from a surface mine in Decker, MT, inoculum from a USGS well in the Powder River Basin, synthetic CBM produced water (main ingredients magnesium, potassium, calcium, ammonium, (as chloride), sodium bicarbonate, experiment started 9/10/2010.

Experiment 2. Decker coal, same inoculum, Synthetic CBM water plus sulfate, started 5/4/2011,

Experiment 3. Decker coal, filtered CBM produced water from a USGS well, Same Inoculum. Started 4/5/2012

ZERT Zero Emissions Research and Technology

MONTANA STATE UNIVERSITY

Lab Results:
Biostimulation of methane production from coal

- Batch systems with native PRB microbes
- Increased methane with algae extract

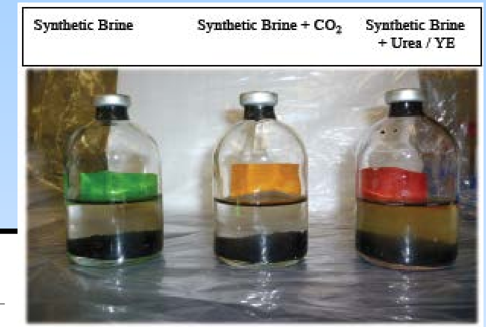

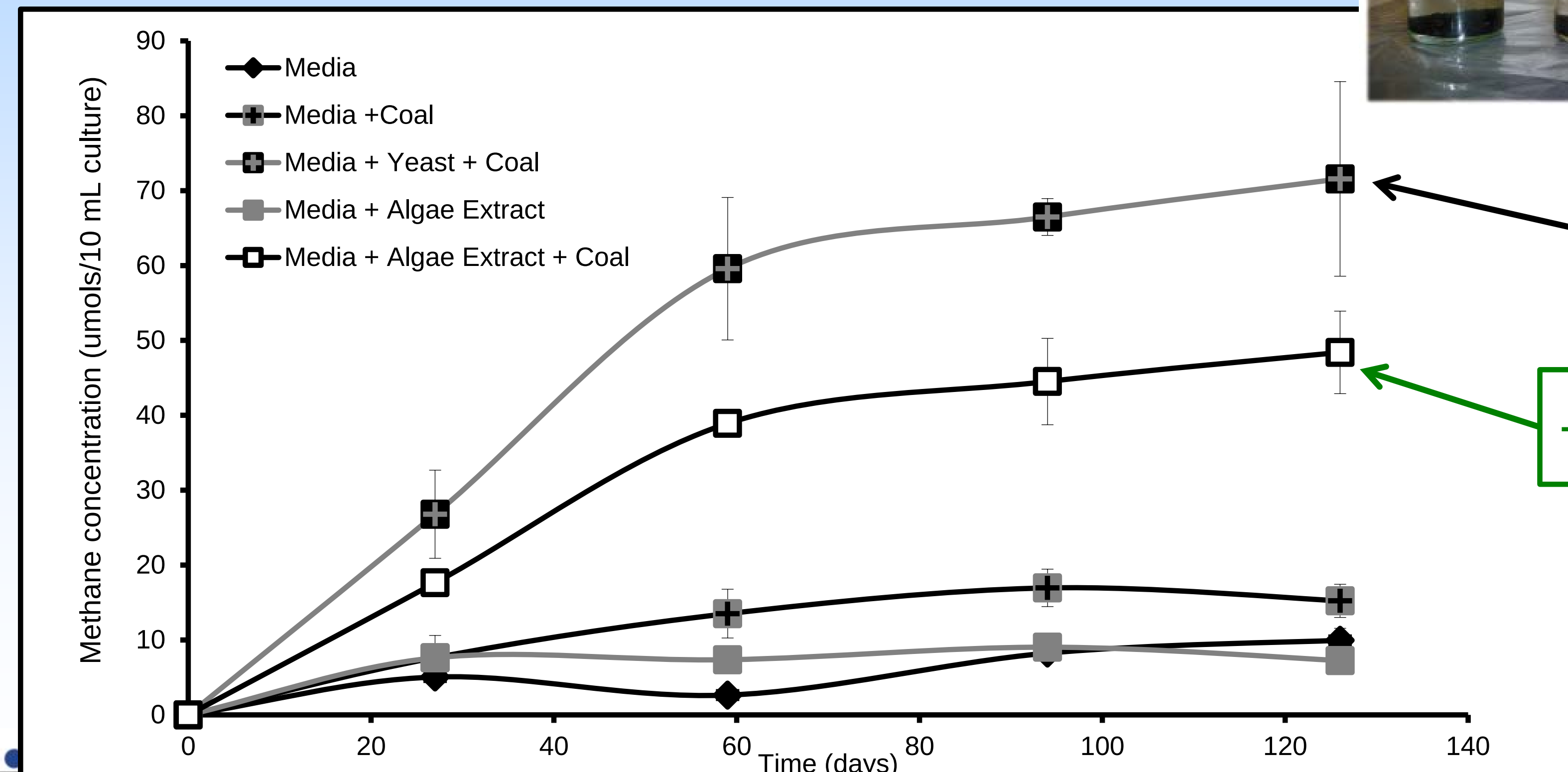

+ Yeast

+ Algae

Barnhart *et al.* in prep

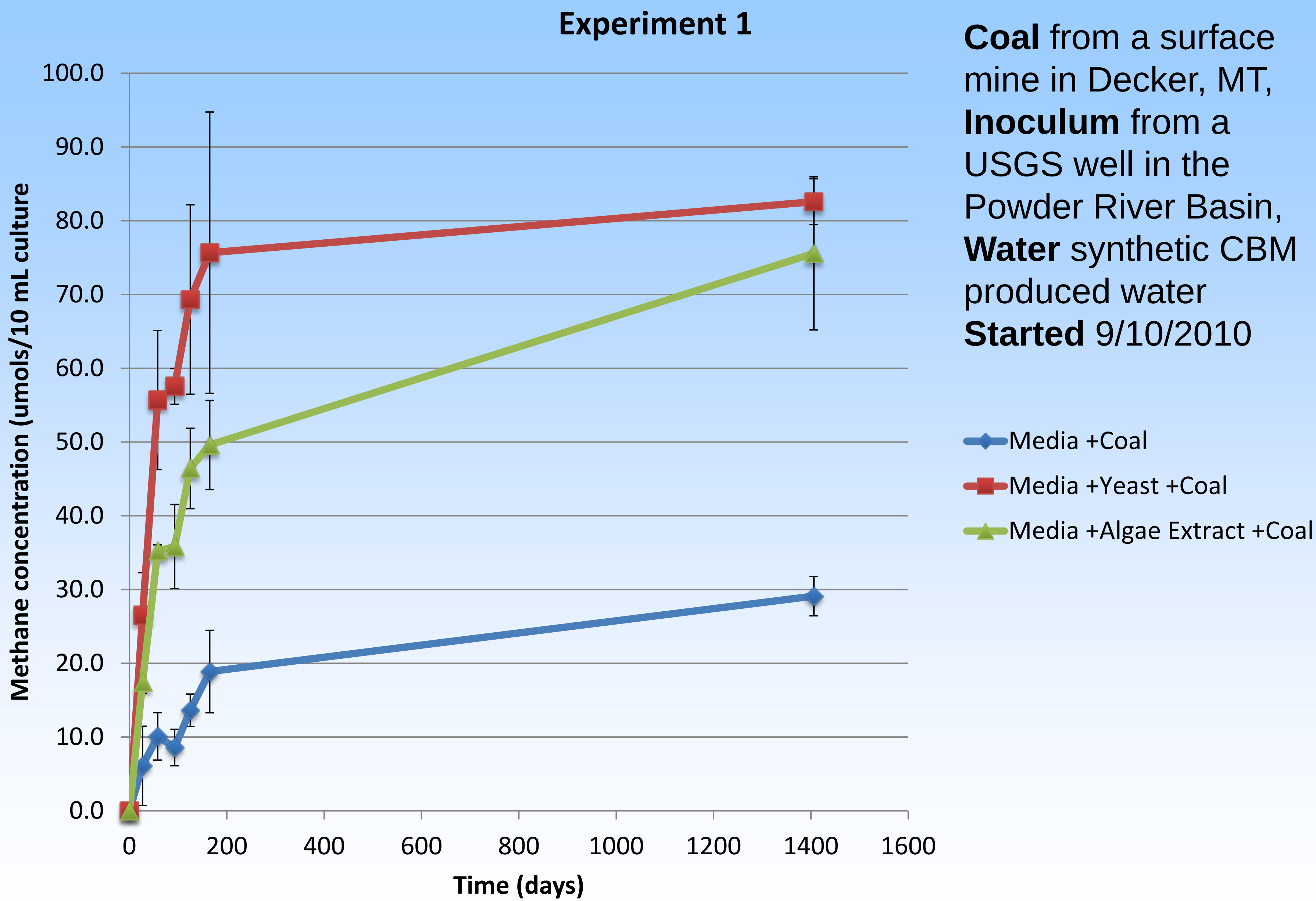

Coal from a surface mine in Decker, MT,
Inoculum from a USGS well in the Powder River Basin,
Water synthetic CBM produced water
Started 9/10/2010

Zero Emissions Research and Technology

MONTANA STATE UNIVERSITY

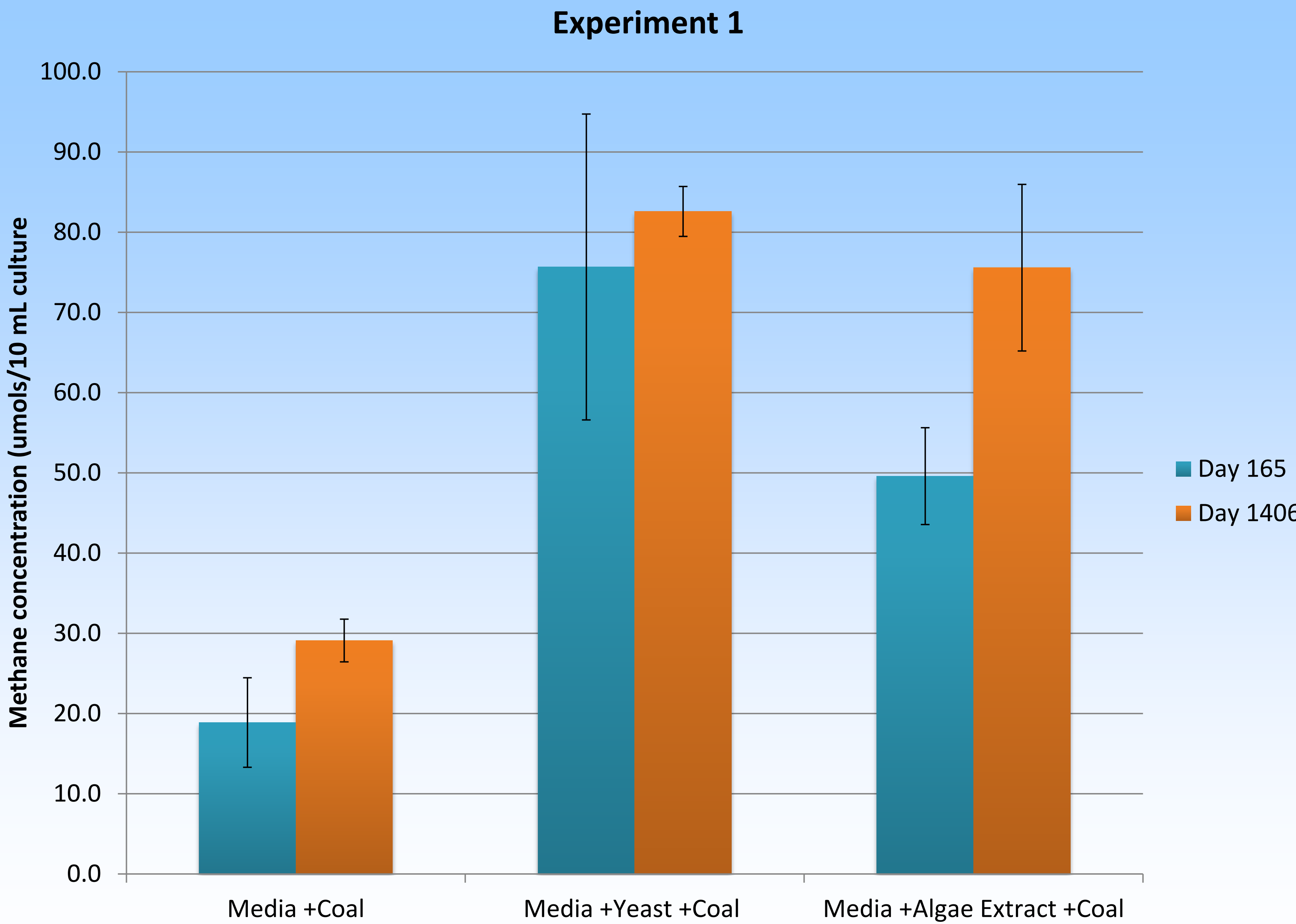

Coal from a surface mine in Decker, MT, **Inoculum** from a USGS well in the Powder River Basin, **Water** synthetic CBM produced water

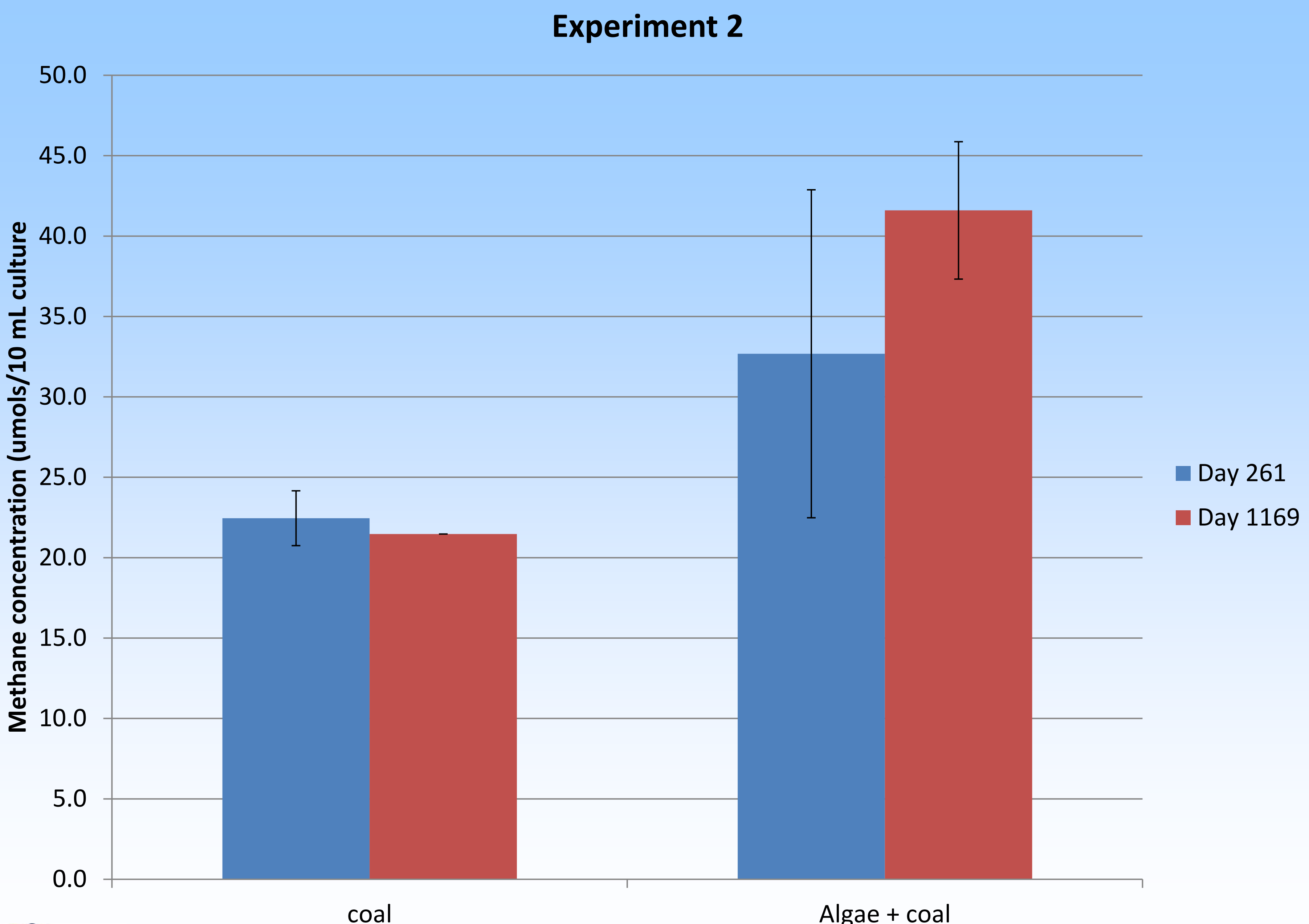

Coal from a surface mine in Decker, MT, **Inoculum** from a USGS well in the Powder River Basin, **Water** synthetic CBM produced water **+ Sulfate**

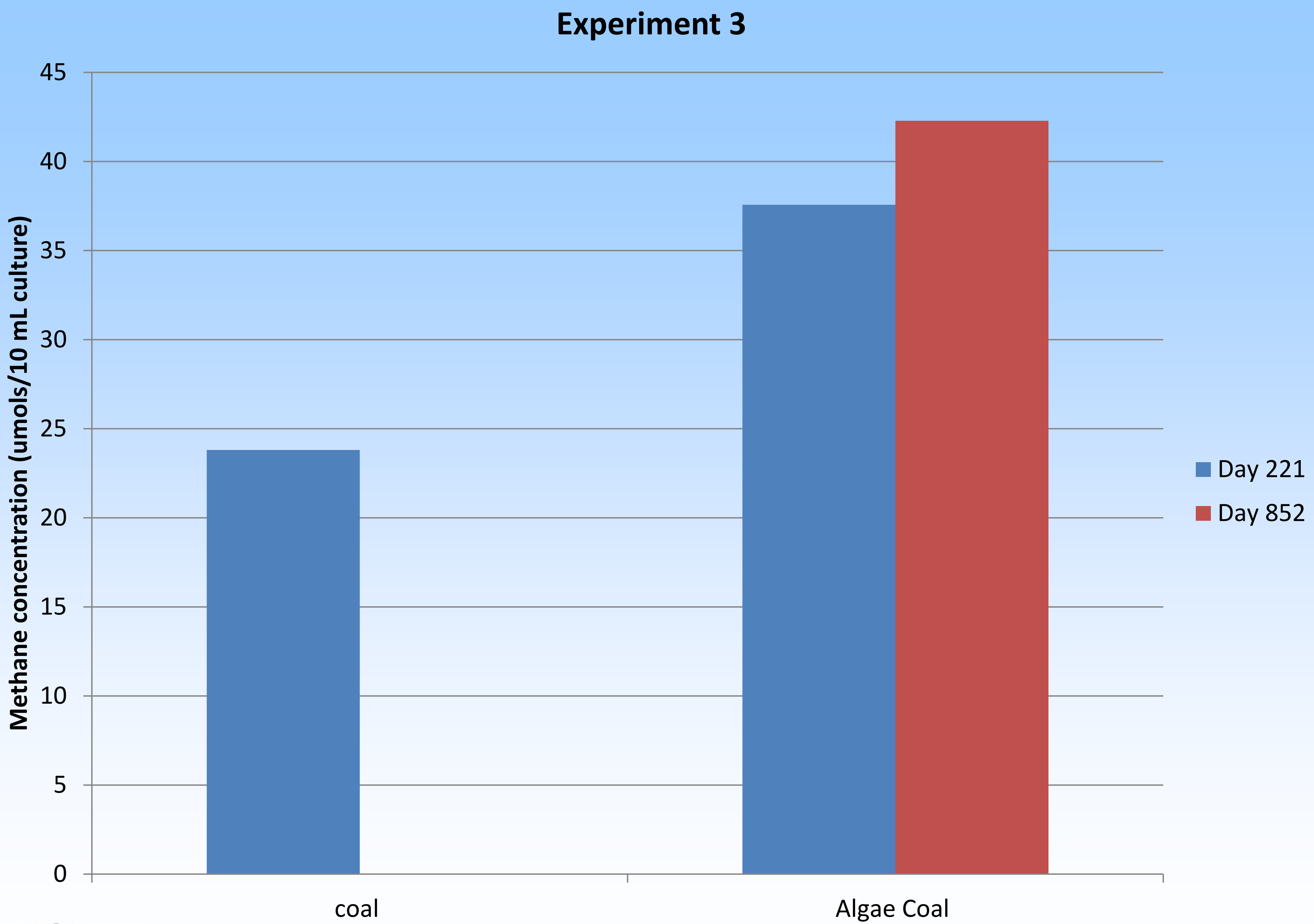

Coal from a surface mine in Decker, MT, **Inoculum** from a USGS well in the Powder River Basin, **Water** filtered CBM produced water from USGS well

Fall 2013 drilling and sampling program in the Flowers-Goodale coal horizon near Birney MT. Coal samples were recovered along with samples of produced water from the coal seam

Elliott Barnhart
Ph.D. Candidate, Microbiology
Center for Biofilm Engineering
USGS – Pathways student

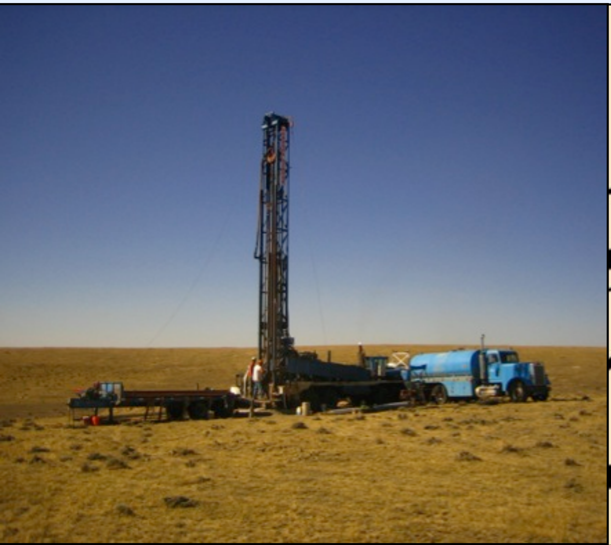

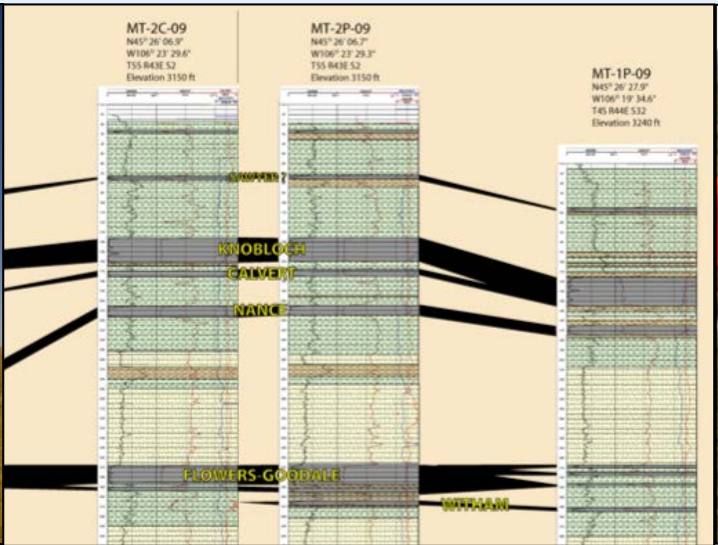

Microbial inoculum samples were recovered from Flowers-Goodale coal in June 2014 using Diffusive Microbial Sampler (DMS)

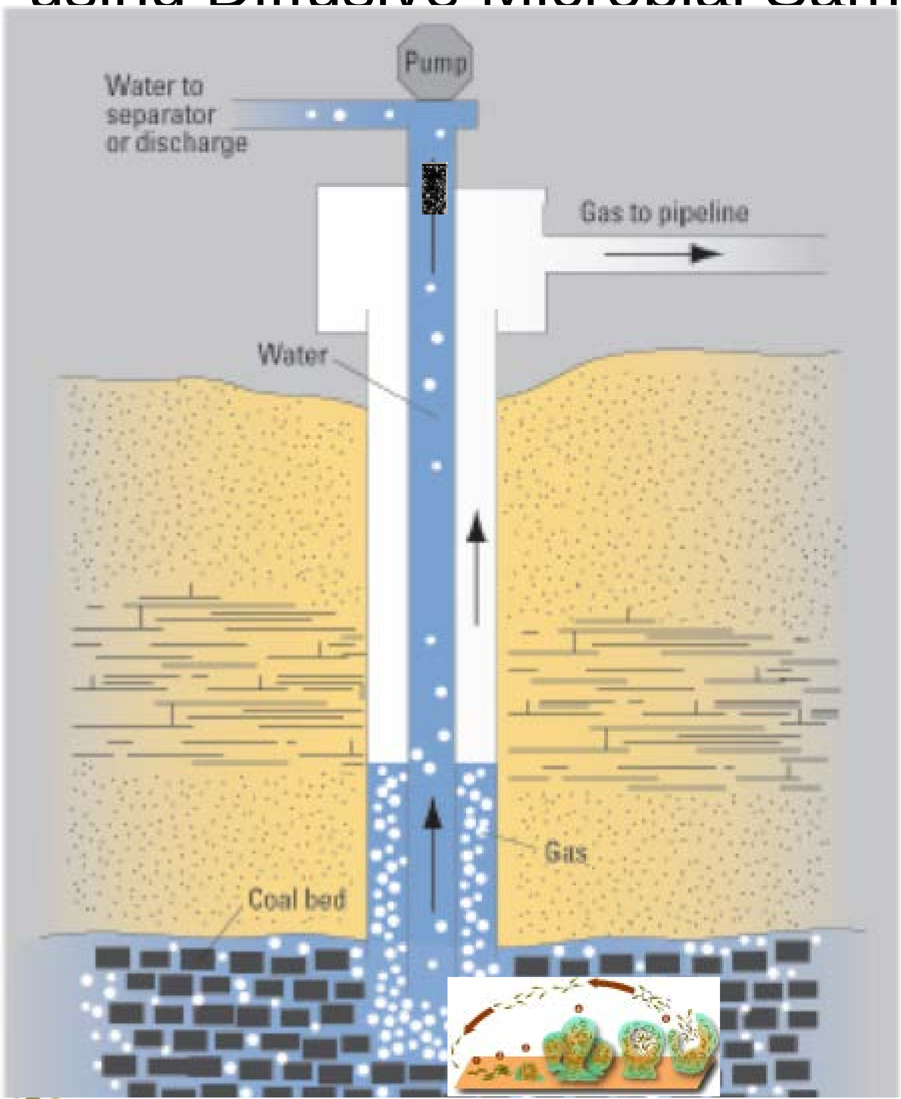

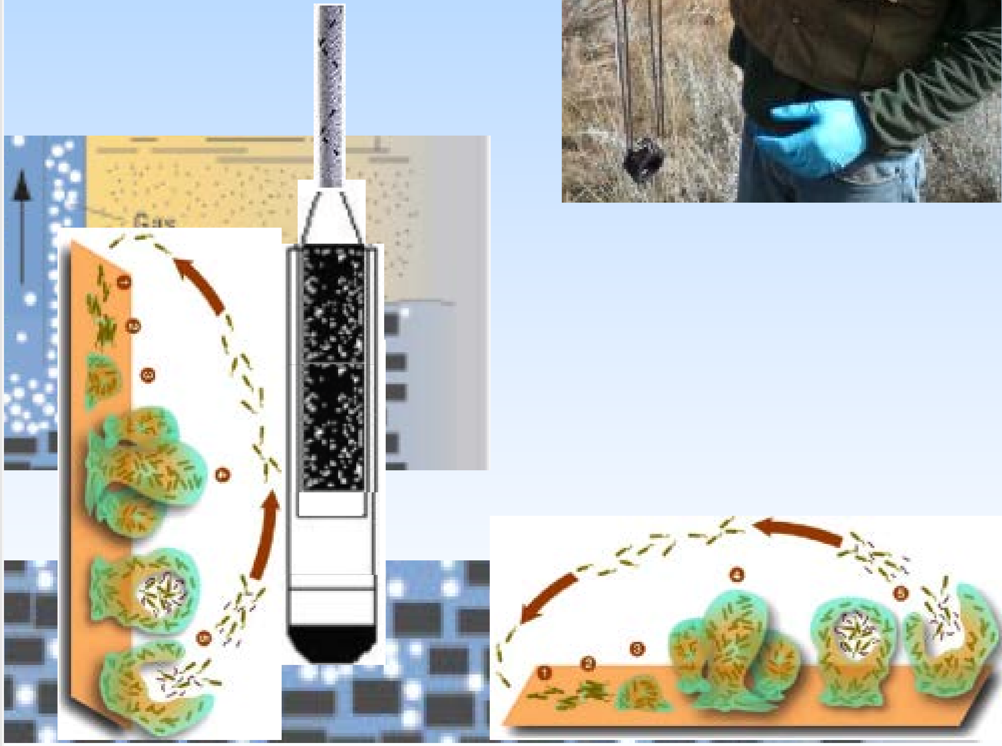

Large Number of Participants / Methods

47 investigators
31 instruments / sensor arrays
5 univ. 6 DOE labs, 4 companies

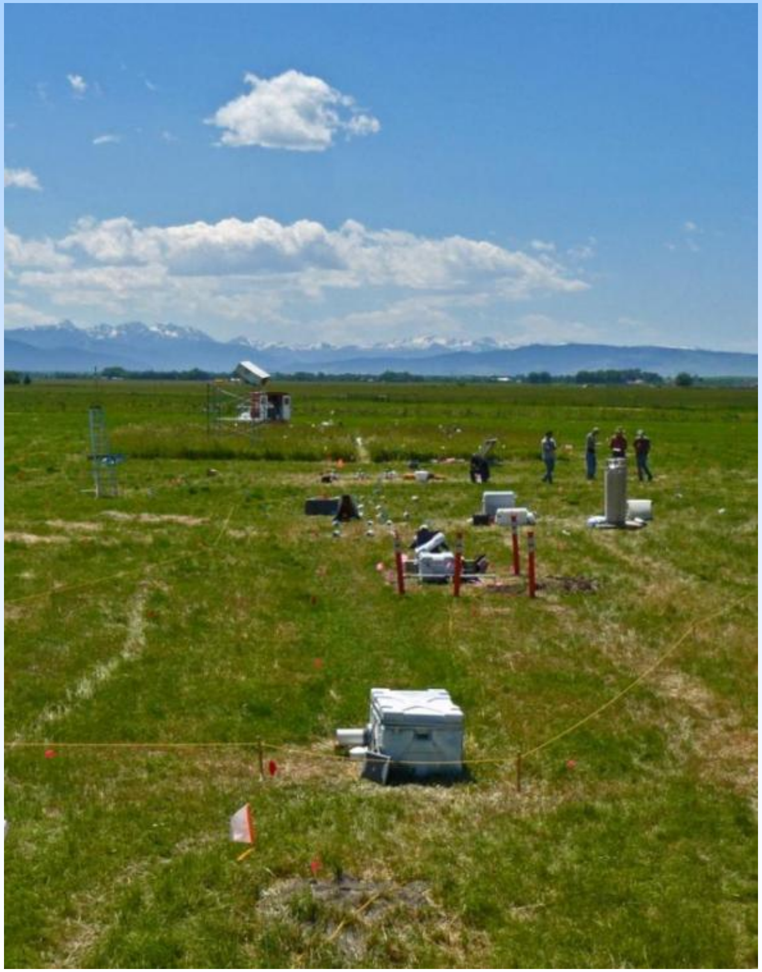

Investigator	Institution	Monitoring Technology	Number of Sensors
Arthur Wells Rod Diehl Brian Strasizar	National Energy Technology Laboratory	Atmospheric tracer plume measurements	1 tower (4m) Blimp (Apogee Scientific) with 3 tether line samplers
		Bee hive monitoring for tracer with sorption tube and pollen trap	2 hives
		Automated Soil CO_2 flux system	4 chambers
William Pickles Eli Silver Erin Male	University of California- Santa Cruz	Hand held hyperspectral measurements (plant health)	1 instrument
Yousif Kharaka James ThordsenGil AmbatsSarah Beers	United States Geological Survey*	Ground water monitoring	1 EC and temperature probe, Dissolved oxygen probe, lab analysis of water samples
Henry Rauch	West Virginia University	Water monitoring well headspace gas sampling	1 sensor
Lucian Wielopolski Sudeep Mitra	Brookhaven National Laboratory*	Ineleastic neutron scattering (total soil carbon)	1 instrument
Martha Apple Xiaobing Zhou Venkata Lakkaraju Bablu Sharma +2 students	Montana Tech*	Soil moisture, temp. Chlorophyll Content Meter , Fluorescence Meter , LI-COR 2000 to measure leaf area index Leaf Porometer to measure stomatal conductance	5 sensors
		Infrared radiometry (plant health)	2 instruments
		Atmospheric humidity and temperature, accumulated rainfall	1 sensor each
		Plant root imaging	1 camera
		Soil conductivity	1 sensor
		Handheld hyperspectral measurements (plant health)	1 instrument
William Holben Sergio Morales	University of Montana*	Microbial studies	Lab analysis

ZERT Zero Emissions Research and Technology

Large Number of Participants / Methods

Investigator	Institution	Monitoring Technology	Number of Sensors
Lee Spangler Laura Dobeck Kadie Gullickson	Montana State University	Water content reflectometers (soil moisture)	15 sensors
		Automated soil CO_2 flux system	5 long term chambers, 1 portable survey chamber
		CO_2 soil gas concentration	6 sensors
Kevin Repasky (PI) Jamie Barr	Montana State University	Underground fiber sensor array (CO_2 soil gas concentration)	4 sensors
Rand Swanson	Resonon*	Flight based hyperspectral imaging system	1instrument
Joseph Shaw (PI) Justin Hogan Nathan Kaufman	Montana State University	Multi-spectral imaging system (plant health)	1instrument
		Meteorological measurements	1 tower
Julianna Fessenden +3 students	Los Alamos National Laboratory	In situ (closed path) stable carbon isotope detection system	1 instrument
		Flask sampling for in situ isotope detection	Lab analysis
Sam Clegg Seth Humphries	Los Alamos National Laboratory	Frequency-modulated spectroscopy (FMS) open-air path	1 instrument
Thom Rahn	Los Alamos National Laboratory	Eddy covariance	1 tower
James Amonette Jon Barr	Pacific Northwest National Laboratory	Soil CO_2 flux (steady-state)	27 chambers
Sally Benson (PI) Sam Krevor Jean-Christophe Perin Ariel Esposito Chris Rella (Picarro)	Stanford University* / Picarro Instruments*	Commercial cavity ringdown real-time measurements of $\delta^{13}C$ and CO_2 in air	1 instrument
Greg Rau Ian McAlexander (LGR)	Lawrence Livermore National Laboratory /Los Gatos Research*	Commercial cavity ringdown real-time measurements of $\delta^{13}C$ and CO_2 in air	1 instrument
Jennifer Lewicki	Lawrence Berkeley National Laboratory	CO_2 soil gas concentration	8 sensors
		CO_2 atmospheric concentration	2 sensors
		Chamber soil CO_2 flux measurements	1 instrument
		Meteorological	1 tower

ZERT Zero Emissions Research and Technology

Flux Chamber

J.L. Lewicki

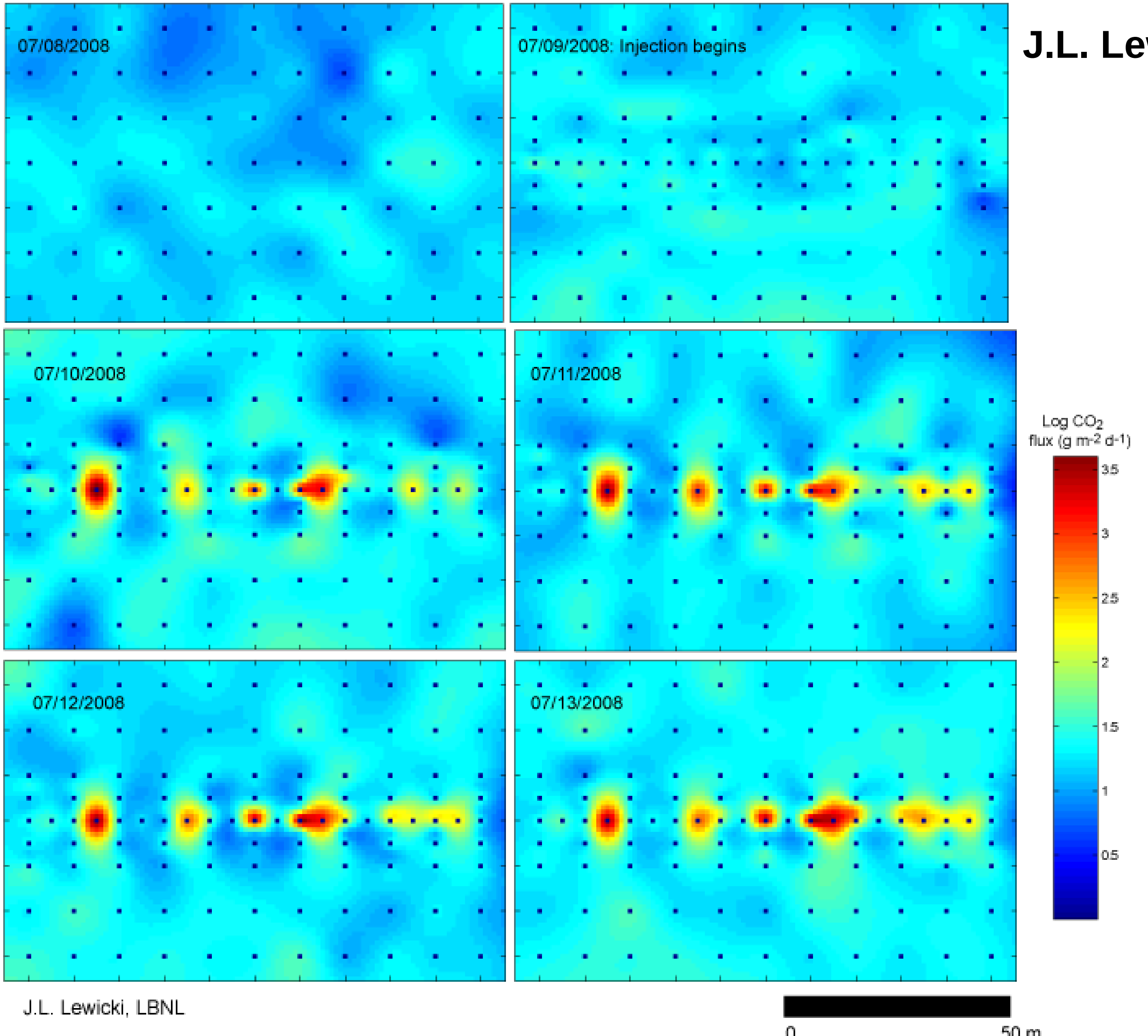

Accomplishments to Date

- Modified two computational codes used for CO_2 simulations
- Studied multiple analogs to inform risk assessment
- Developed and performed initial field tests on three prototype moderate area near surface detection technologies
- Performed studies to deepen understanding of capillary trapping mechanism
- Hosted other academic institutions, gov. agencies and private sector entities in field experiment

Accomplishments to Date

- We have demonstrated biomineralization sealing of fractured shales achieving four orders of magnitude permeability in fractures with several mm apertures.
- Methods for monitoring biogenic methane production from coal have been successfully developed and three sets of long term coal-to- methane experiments are on-going.
- We now have the capability to study biogenic coal-to-methane conversion using coal samples, formation water, and microbial inoculum from the same location (Flowers-Goodale coal layer near Birney MT
- An MRI-compatible core holder and new pulse sequence enables us to: 1) Observe water in real, porous rock cores, 2) Inject liquids, gases, or supercritical fluids (brine, CO2, etc.) 3) Acquire 3D images and 4) Observe transport and structural changes in situ in ~50 sec. with ~1 mm resolution
- Achieved strain sensitivity for a fiber sensor of 60×10^{-9}. Next step is to develop non-Bragg grating technique for downhole distributed seismic sensing

ZERT Zero Emissions Research and Technology

MONTANA STATE UNIVERSITY

Summary

– Key Findings Enrichnent of coal microcosm experiments with Algae extract and ____resulted in increased methane production of ____to___% compared to the same coal with out AE. These findings suggest that algae can be farmed in produced water impoundments, processed for biofuel production, and the extract used on-site to stimulate additional methane production underground. Algae farming will increase the CO_2 uptake from the atmosphere thereby reducing the carbon footprint of the overall CBM operation.

– Lessons Learned There are many factors which affect the rate of biogenic methane production in laboratory microcosm experiments including maintaining field-relevant redox conditions and water chemistry. Utilizing samples of inoculum, formation water and coal from the same coal formation will minimize these and other related problems.

– Future Plans Batch microcosm experiments will continue. We are also beginning the design of flowing column coal-to-methane conversion experiments to assess methane production kinetics under representative groundwater flow conditions.

ZERT Zero Emissions Research and Technology

MONTANA STATE UNIVERSITY

What We Have Learned

- Many near surface methods are quantitative <u>but</u>
  - Diurnal, seasonal, annual variations in ecosystem background flux affect detection limits
  - Appropriate area integrated, mass balance is a challenge
- Nearly all methods could detect 0.15 tonnes / day release at ZERT site.
- Scaling, 6 tonnes per day would be detectable over an area 40 times as large
- Surface expression was "patchy" – 6 areas of ~5m radius
- Natural analogs also seem to have "patchy" surface expression

MONTANA STATE UNIVERSITY

Summary

- Multiple computational codes have been improved
- Near surface detection technologies have been tested
- Analogs are providing important information to understanding of risk

ZERT II

Natural Analogs of CO_2 Escape Mechanisms
Pryor Mountain and Big Snowy study areas
Carbon Storage R&D
Slides

Big Snowy Mountains Field Area

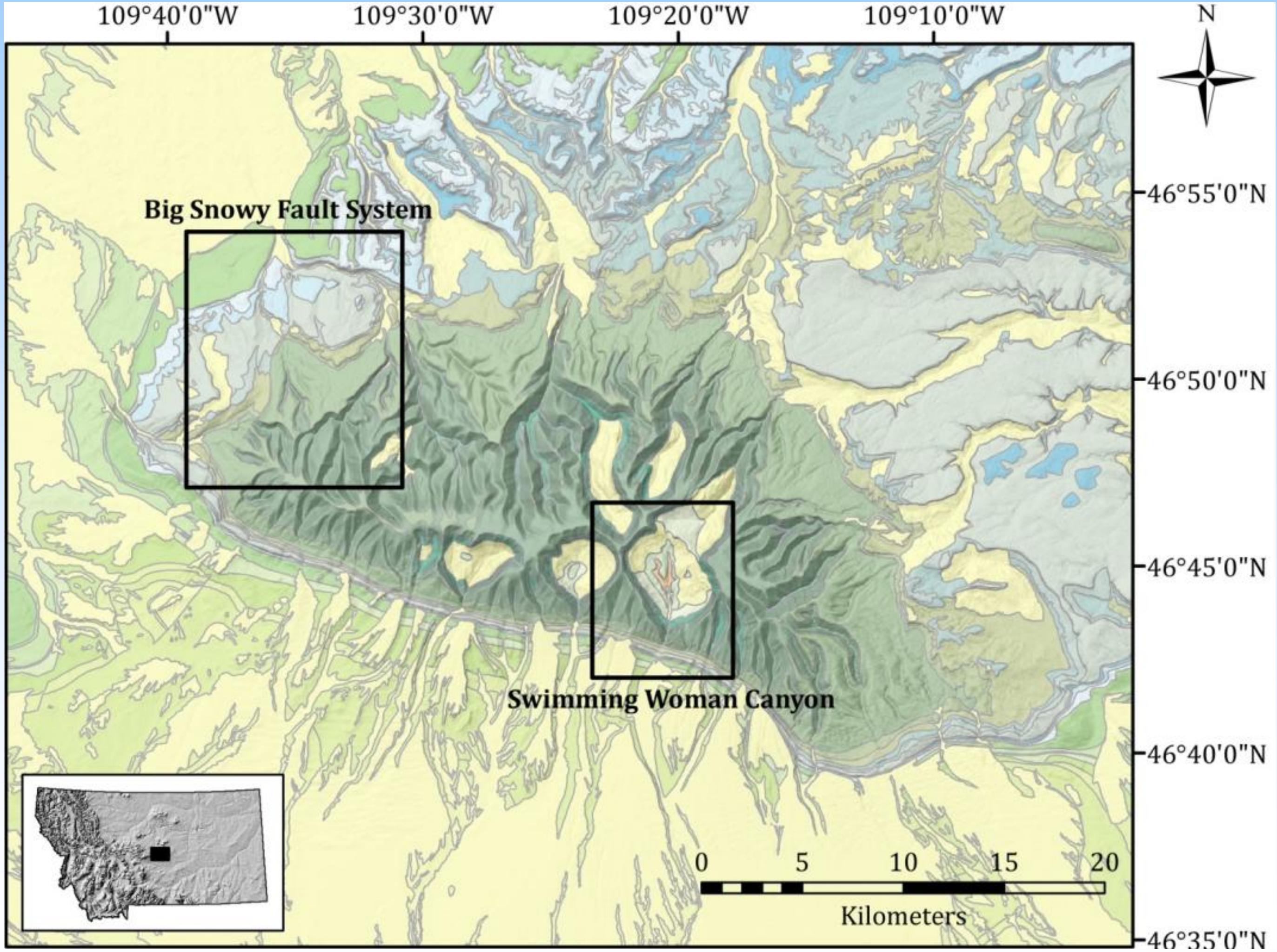

Pryor Mountain Study Area

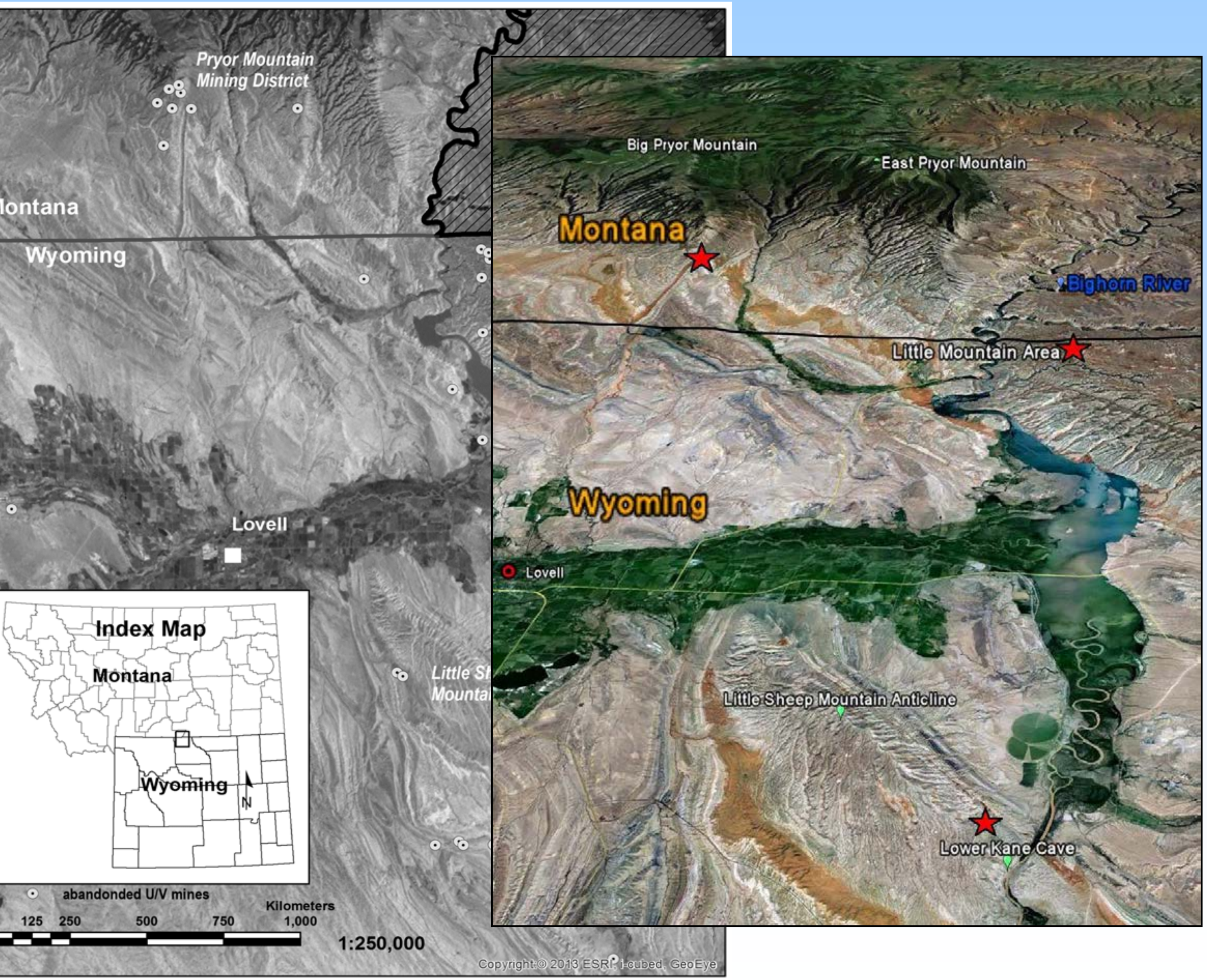

Favorable sites for Hydrothermal Dolomite formation

A. Cartoon figure of paleohighs and strike slip faults showing favorable sites for hydrothermal dolomite formation, figure adapted from Davis and Smith, 2006. The Pryor Mountains are divided N - S by the Nye-Bowler lineament a major sinistral strike slip fault and the Snowy Mountain Study area has a strike slip faults which may source migrating fluids. Little Sheep Mountain and Little Mountain areas formed over paleohighs which influence the fracture density and may concentrate fluid flow in these areas.

B. Cartoon figure showing greater fault intensity in paleokarst situated over paleohigh, figure adapted from Eldam, 2012. t_1 and t_2 (green boxes) represent fracture intensity/density before and after uplift. The small arrow beneath the high could correspond to the location of the fault in the core of Little Sheep Mountain and be an area of concentrated fluid flow and breccia formation in the Madison Limestone a reservoir rock being considered in some carbon sequestration sites.

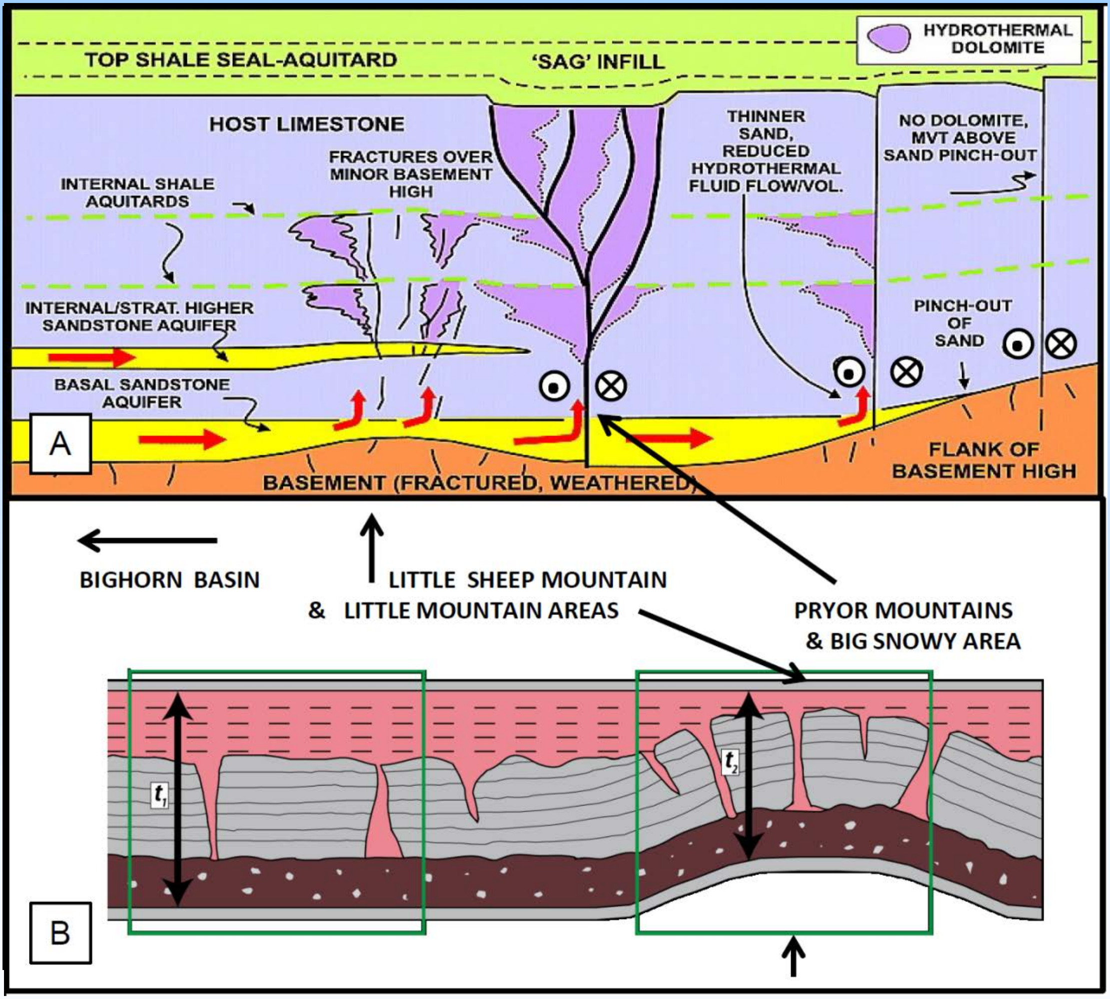

Model for the formation and fluid source of a hydrothermal breccia pipe

A. Fluid Migration Pathways In this model, hydrothermal fluids are sourced by a combination of meteoric and basement fluids that flow along pre-existing structures in the subsurface. Hydrothermal fluids rise along pre-existing structures, preferentially hydrofracturing the hanging wall side of features (modified from Huntoon, 1993; Katz et al., 2006)

B. Formation of Breccia Bodies Brecciation continues along the thrust sheet, forming shatter breccias in an increasingly vertical pattern. In both cases, hot fluids rise through strata in unpredictable patterns, creating off-shoots near sequence boundaries due to major changes in mechanical properties (modified from Katz et al., 2007). Depleted $\delta^{18}O$ and $\delta^{13}C$ in late-stage calcite and dolomite precipitated along brecciated zones and fracture systems in Mississippian limestone the Pryor Mountain and Big Snowy study areas are fingerprints of these processes. These areas are major avenues of enhanced porosity and permeability in the subsurface and have important applications at some sites in Montana where carbon sequestration is under consideration.

C. Similar model for the formation of hydrothermal breccia pipes. Hydrofracturing at the fault tip results in three stages of progressively damaged and mineralized zones. These stages include (a) a zone of permeation at the propagating fault tip, causing extensive hanging wall dolomitization; (b) a region of hydraulic fracturing and brecciation of the previously dolomitized halo, resulting in the precipitation of hydrothermal minerals; and (c) the repetition of seismic events, allowing the brecciated area to become progressively more vertical with continued activity (modified from Phillips, 1972; Davies and Smith, 2006; Jeffrey, 2014).

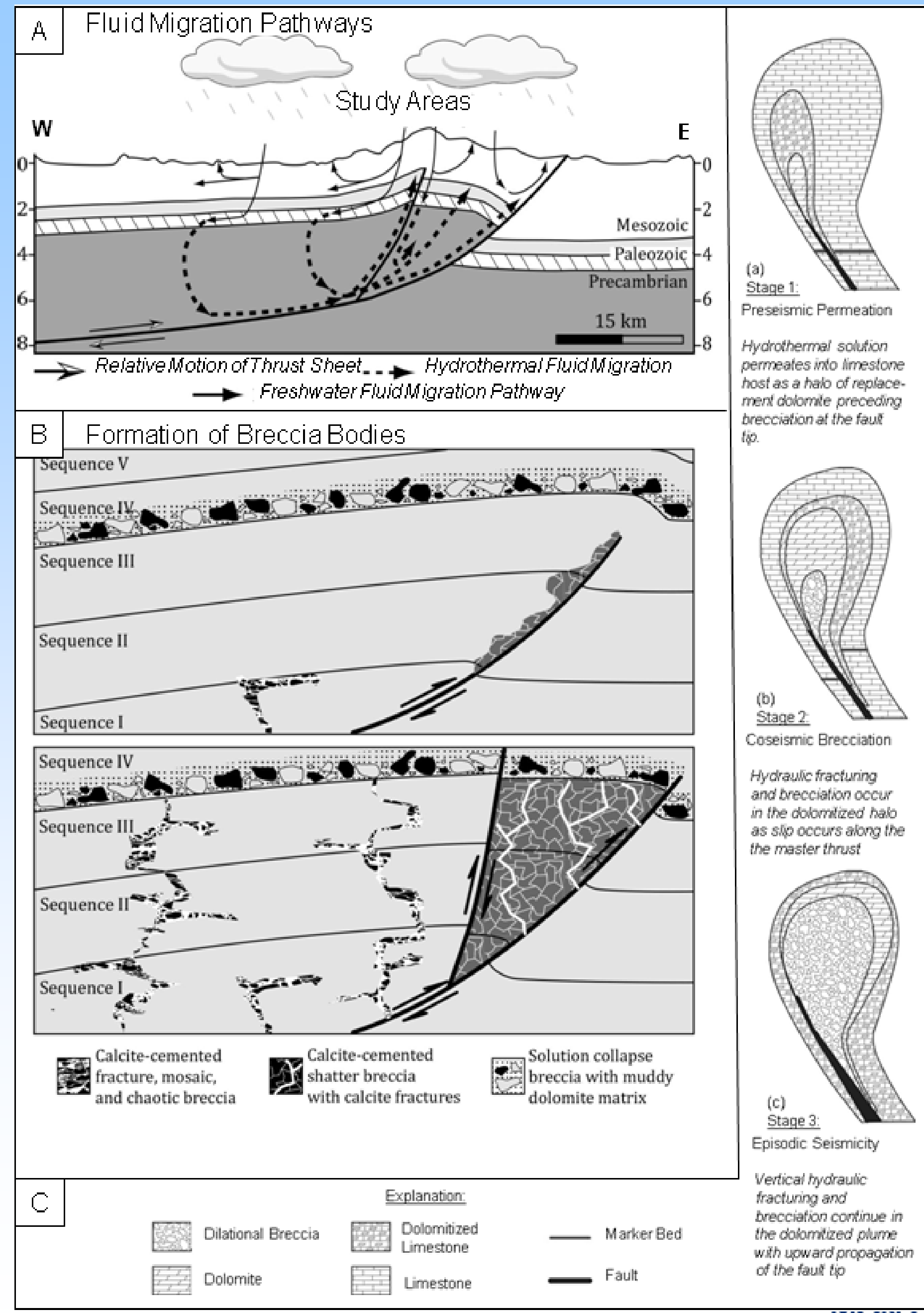

Hydrothermal Breccias and fluid flow examples in Little Sheep Mountain, WY

A. Hydrothermal breccia formed along an oblique to strike fracture in Madison Limestone in the LSMA. Note bleached rock along fracture and bedding planes.

B. Small dolomitized, possibly silicified breccia pipe protruding from roof of Lower Kane Cave.

C. Sample LSM-RRC008 silicified floating clast breccia near Lower Kane Cave. Matrix sampled has a $\delta^{18}O$ value of -11.07 and $\delta^{13}C$ value of 0.02 reflecting warm fluid migration.

D. Oil impregnated breccia clast from Little Sheep Mountain. SM-RRC001 sample location. Three samples were analyzed from this site for stable C and O isotopes: LSM-00l a silicified Permian limestone had the most depleted $\delta^{18}O$ value of -14.09 and the most depleted $\delta^{13}C$ value of all the samples in the Pryor Mountain study area of -10.31.

E. Gypsum coated breccia Lower Kane Cave. The walls have dried bitumen which seeped along breccia clasts and along fractures. Twenty centimeter arrow for scale is in lower portion of photo.

F. Hydrothermal breccia which may be associated with the breccias in Lower Kane Cave (B above) has a $\delta^{18}O$ value of -12.80 and $\delta^{13}C$ value of -0.03. Breccia formed along oblique to strike of the anticline axis fractures bleaching is evident on the side of the breccia.

ZERT Zero Emissions Research and Technology

MONTANA STATE UNIVERSITY

Stable O and C Isotope Data
Madison & Permian Limestone

A. Stable carbon and oxygen isotope analyses data from brecciated host rock and vein fill material from the Pryor Mountain Study area. The black symbols are from the Little Mountain area and the Pryor Mountains. The red and blue symbols are from Little Sheep Mountain. Squares are host rock, triangles vein fill material., circles breccias and crosses are the standards which are circled in the figure. The dashed boxes represent approximate value for Mississippian and Permian seawater carbonate based on Veizer et al., 1999. The oval shape shows the most depleted $\delta^{13}C$ and $\delta^{18}O$ values are mainly the late stage vein fill material and breccias.

B. Carbon and oxygen graphs of Phanerozoic $\delta^{13}C$ and $\delta^{18}O$ trend. Carbon is for combined Bochum/Ottawa (based on 1564 brachiopod (secondary layer) and belemnite (laminae pelucidae) measurements at Bochum and Ottawa and literature data (compiled from 3918 measurements for low Mg calcite (brachiopods, belemnites, oysters, foraminifera) and 96 measurements for aragonite (mollusk shells). The running mean is based on 20 Ma window and 5 Ma forward step. The shaded areas around the running mean include the 68% (+/- 1σ for a strictly Gaussian distribution) and 95% (+/- 2σ) of all data (From Veizer et al., 1999 and references within). Dashed boxes are values represented in top graph.

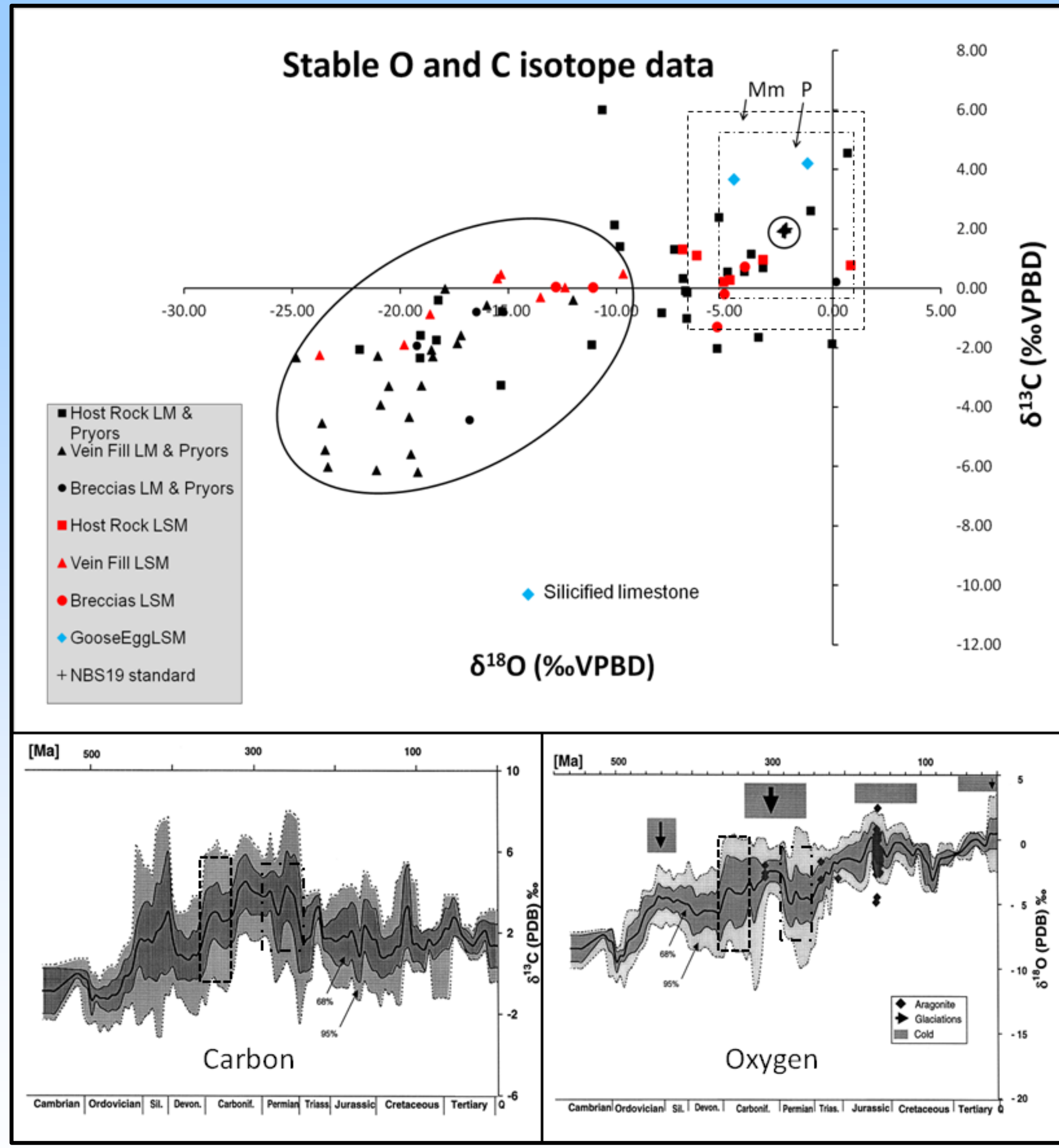

Porosity change accompanies brecciation and dolomitization

SEM and BoneJ analyses of matrix material from breccias A & B highlight the amount of porosity present. SEM images were used to determine secondary porosity associated with matrix dolomitization, which was too fine to see through petrographic analysis. The Mission Canyon Formation in the Snowy Mountain study area is characterized by poor intrinsic porosity and permeability; however, in brecciated regions matrix material of the Mission Canyon Fm. added a strong secondary fabric to the rock, creating open vuggy space and intercrystalline porosity.

SEM (left) and the BoneJ plug-in of ImageJ (right) analyses were of matrix material from breccias located along the Big Snowy fault system. SEM images (greyscale) were analyzed using a color thresholds (light blue) highlighting the amount of porosity present. Such two-dimensional area calculations suggest that pore space increased by **5-25%** as a result of hydrothermal brecciation.

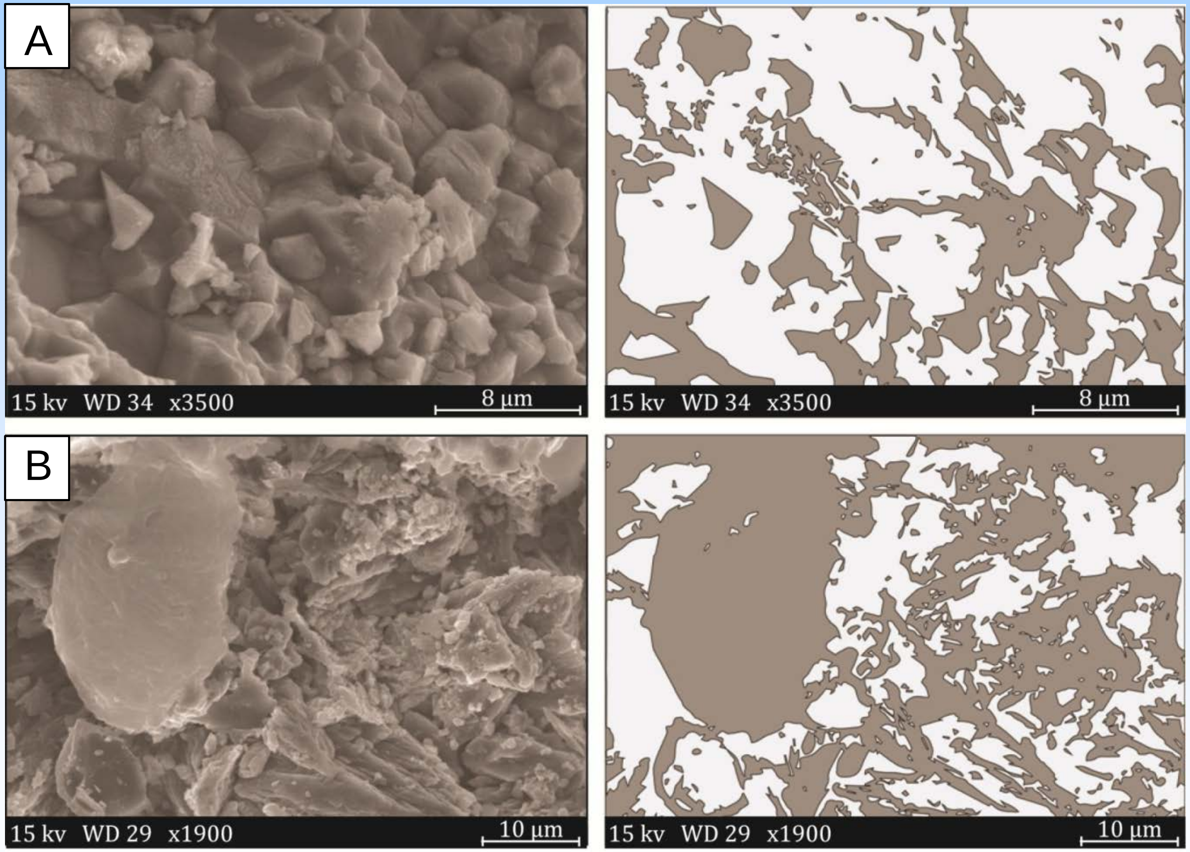

Figure from Jeffrey, 2014

Hydrothermal brecciation characterized by multiple episodes of fluid flow

A. Breccia with boxwork texture

B. Thin section of stained breccia with late stage calcite (pink), bitumen (black) and purple fluorite filling in void space created during brecciation.

C. Cathodoluminescence image of fracture fill **shows multiple episodes of fluid migration with iron rich, darker bands alternating with regular late stage calcite.**

D. Breccia with vugs filled with dark purple to black fluorite.

E. Inset SEM image of a corroded fluorite crystal, 1000x magnification

F. F. & G. Large silicified, dolomitic floating clast breccia Red Pryor Mountain; clast (F) was cut, polished and stained for carbonate identification. The matrix is ferroan dolomite and there were at least two late stage calcite vein filling episodes. The last was ferroan calcite. The sample was drilled for isotope analyses from the veining and the matrix. The late stage ferroan calcite was the most depleted in $\delta^{18}O$ with a value of -15.99 and a $\delta^{13}C$ value of -0.40. The clast shows fractures healed by calcite (arrow) and later fracturing along edge of clast and through matrix.

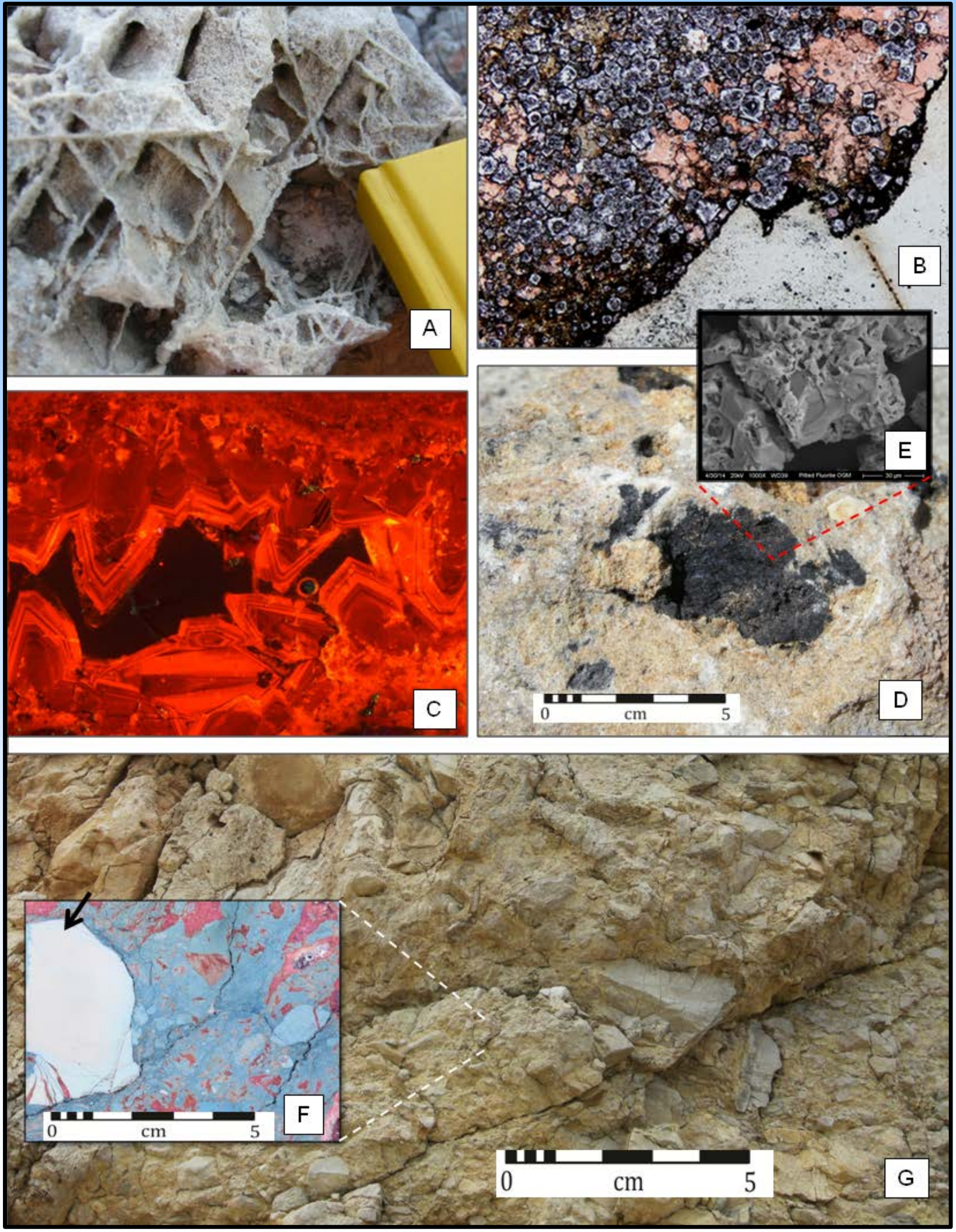

Zero Emissions Research and Technology

MONTANA STATE UNIVERSITY

Some factors for CO_2 Reservoir Characterization in Paleozoic reservoir rocks

- Porosity and permeability may be influenced by tectonic hydrothermal breccias:
  - Heterogeneity is created by hydrothermal breccias which may serve to increase porosity or occlude it.
  - Dolomitization may increase the porosity while late stage calcite may serve to occlude it.
  - Faulting and brecciation within perspective reservoir units must be thoroughly characterized for such secondary networks of permeability, as they create unpredicted anisotropy within the reservoir.
- Structural position may influence the flow of fluids in the subsurface.
  - Paleohighs may serve as areas of increased density of fractures and fracture intensity thus increasing porosity and permeability of the fractured units.
  - Preexisting faults, fractures and joints may serve as conduits for the migration of fluids in the subsurface.
  - Position on a structure such as the axis of an anticline vs. the forelimb or backlimb will influence the fluid migration and trapping capabilities of the reservoir system.
- Stratigraphy and mechanical stratigraphy in Paleozoic reservoir rocks may influence fluid migration locally within a unit.
  - Mechanical stratigraphy can influence the migration of fluids in a reservoir rock
  - Thickness of layers within a formation respond differently to applied stress.
    - Thinner units may have greater density of fractures within a stratigraphic unit and provide greater fracture permeability in that unit influencing fluid flow

ZERT Zero Emissions Research and Technology

MONTANA STATE UNIVERSITY

Appendix

– These slides will not be discussed during the presentation, but are mandatory

Organization Chart

- Describe project team, organization, and participants.
  - Link organizations, if more than one, to general project efforts (i.e. materials development, pilot unit operation, management, cost analysis, etc.).

- Please limit company specific information to that relevant to achieving project goals and objectives.

Organization Chart

MSU Internal Management Structure

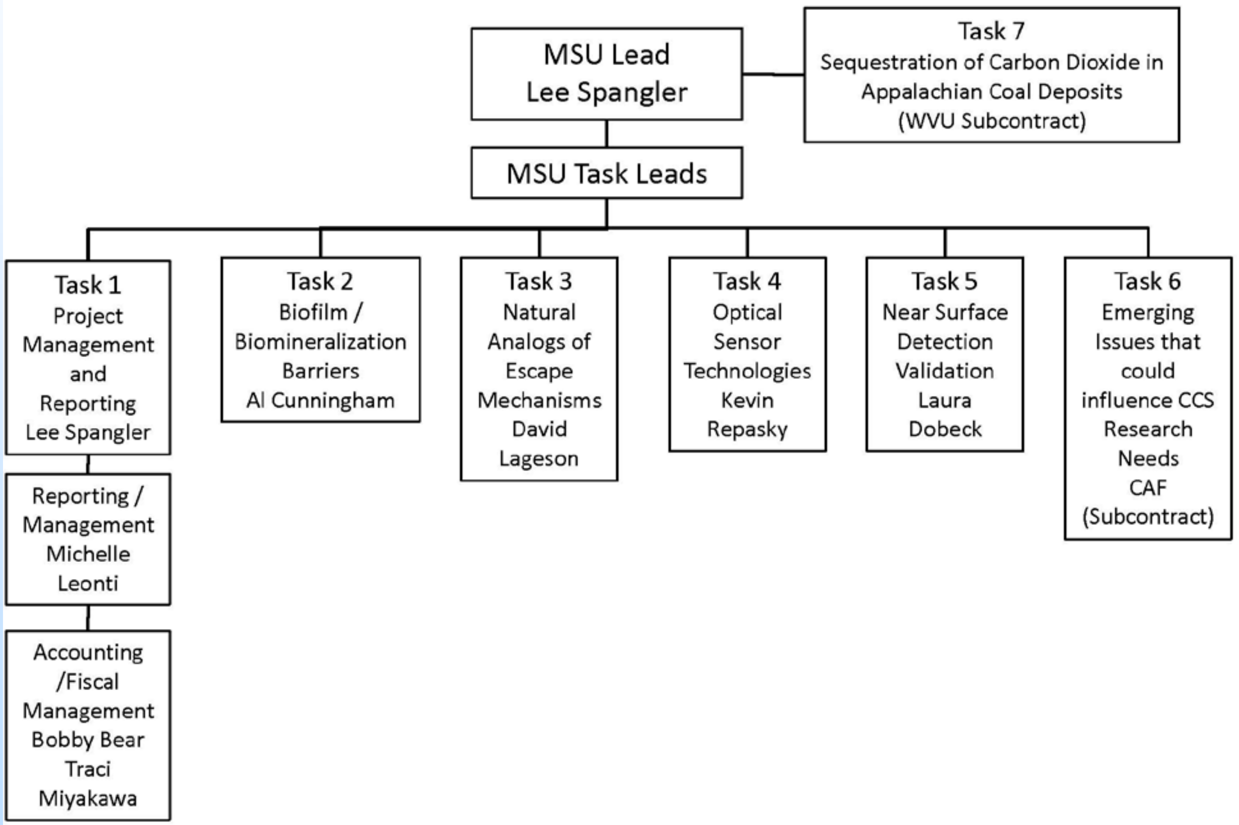

Gantt Chart

- Provide a simple Gantt chart showing project lifetime in years on the horizontal axis and major tasks along the vertical axis. Use symbols to indicate major and minor milestones. Use shaded lines or the like to indicate duration of each task and the amount of that work completed to date.

Gantt Chart

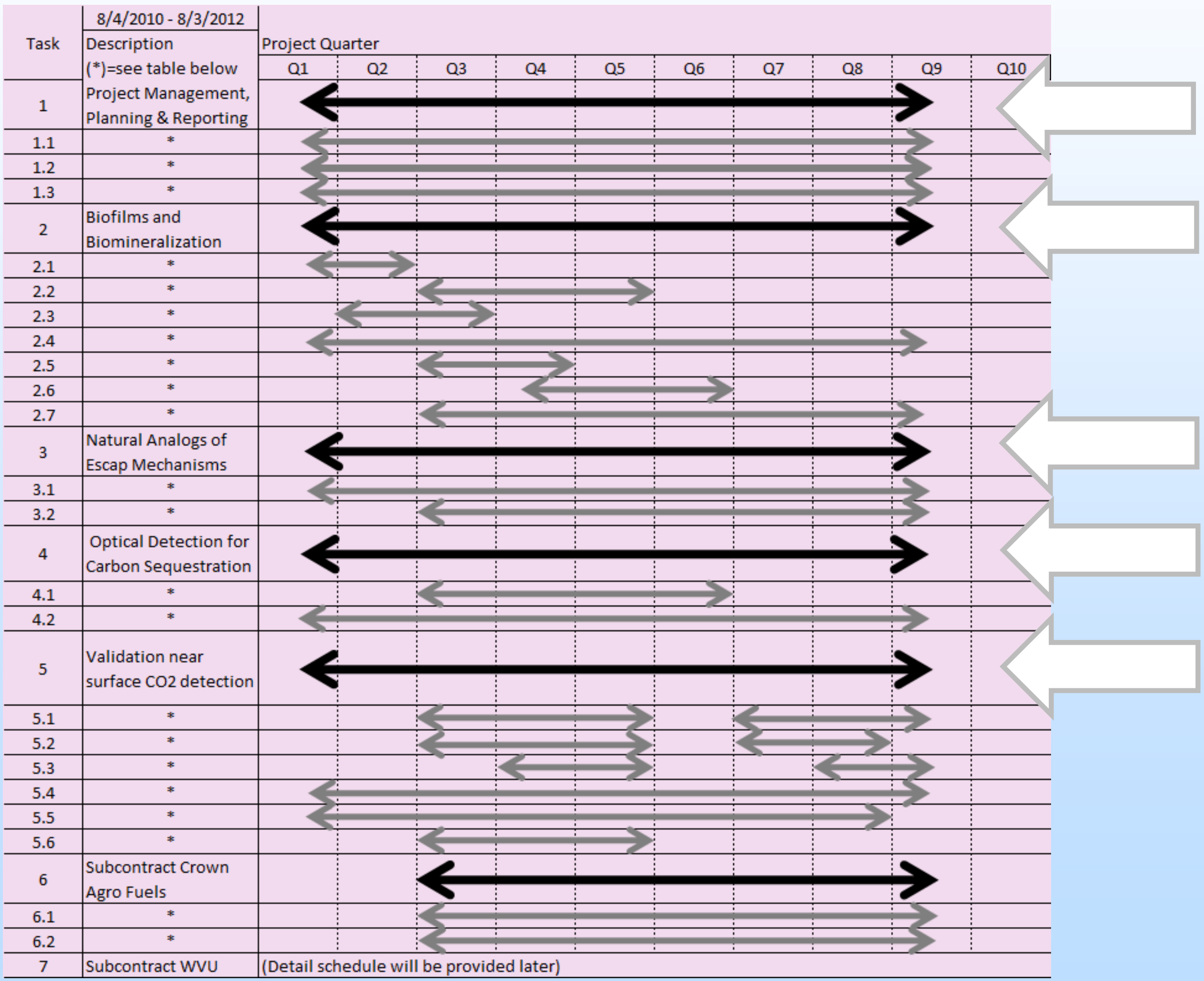

The tasks are continued in the no-cost extension awarded in August 2012.

Gantt Chart

Cont.

Task 1.0 – Project Management, Planning, and Reporting
Subtask 1.1 Project Management
Subtask 1.2 Project Reporting
Subtask 1.3 Presentations and Briefings
Task 2.0 – Biofilms and Biomineralization
Subtask 2.1 Conduct experiments on CO_2 biomineralization deposits on flat coupons and in porous media bead packs.
Subtask 2.2 Develop method to control deposition rate of biomineralized calcium carbonate with distance along a porous media flow path.
Subtask 2.3 Optimize biomineralization of isotopically labeled CO2 carbon under variable head space pressure.
Subtask 2.4 Evaluate the potential for coalbed mediated CO2 sequestration.
Subtask 2.5 Construct a system capable of flowing supercritical fluids through the bore of the magnet of the NMR spectrometer.
Subtask 2.6 Evaluate transport phenomena for brine and supercritical CO2 using magnetic resonance techniques.
Subtask 2.7 Evaluate transport phenomena for brine and supercritical CO2 in a bead pack or other model porous media.
Task 3.0 – Natural Analogs of Escape Mechanisms
Subtask 3.1 Leakage versus Confinement Associated with Subsurface Migration of Natural CO_2 across Faults and Fracture Networks
Subtask 3.2 Ancient Hydrothermal Plumes as a Natural Analog of Hydrofracing Caprocks and Geochemical Healing Mechanisms
Task 4.0 – Optical Detection for Carbon Sequestration Site Monitoring
Subtask 4.1 Underground Fiber Optic Sensors
Subtask 4.2 UltraCompact Thermal Infrared Imagers
Task 5.0 – Validation of Nearsurface CO2 Detection Techniques and Transport Models at Experimental Field Site.
Subtask 5.1 Seasonal Site Preparation
Subtask 5.2 Coordinate experimental season with ZERT team.
Subtask 5.3 Collect data in support of ZERT research project goals.
Subtask 5.4 Investigate opportunities for greater involvement outside of the ZERT team.
Subtask 5.5 Support optical remote sensing group
Subtask 5.6 Support pollen capture of tracers experiments:
Task 6.0 – Tracking Emerging Issues That Could Influence CCS Research Needs
Subtask 6.1 Provide information to government at the state, federal and international levels.
Subtask 6.2 Provide information to NGOs, industry groups, and professional groups relevant to CCS.
Task 7.0 – Sequestration of Carbon Dioxide in Appalachian Coal Deposits (WVU Subcontract)
(Detailed Task and Subtask descriptions will be provided at a later date.)

Bibliography

1. Johnson, J., Shaw, J.A., Lawrence, R.L., Nugent, P., Hogan, J.A., Dobeck, L. and Spangler, L., Comparison of long-wave infrared and visible/near-infrared imaging of vegetation for detecting leaking CO2 gas. IEEE Journal Selected Topics in Applied Earth Observation & Remote Sensing, 2014. 7(5): p. 1651-1657 DOI: 10.1109/JSTARS.2013.2295760
2. Barnhart, E., De Le'on, K.B., Ramsay, B., Cunningham, A. and Fields, M., Investigation of coal-associated bacterial and archaeal populations from a diffusive microbial sampler (DMS). International Journal of Coal Geology, 2013. 115(August 2013): p. 64-70 DOI: 10.1016/j.coal.2013.03.006.
3. Cunningham, A.B., Lauchnor, E., Eldring, J., Esposito, R., Mitchell, A., Gerlach, R., Phillips, Ebigbo, A. and Spangler, L., Abandoned Well CO2 Leakage Mitigation Using Biologically Induced Mineralization: Current Progress and Future Directions. Greenhouse Gases: Science and Technology, 2013. 3(1): p. 40-49 DOI: 10.1002/ghg.1331.
4. Ebigbo, A., Phillips, Gerlach, R., Helmig, R., Cunningham, A.B., Class, H. and Spangler, L., Darcy-Scale modeling of Microbially Induced Carbonate Material Precipitation In Sand Columns Water Resources Research, 2013. 48(W07519) DOI: 10.1029/2011WR011714.
5. Fang, Y., Nguyen, K., Carroll, M., Xu, Y., Yabusaki, T., Scheibe, A. and Bonneville, A., Development of a coupled thermo-hydro-mechanical model in discontinuous media for carbon sequestration. Int. J. Rock Mech. Min. Sci., 2013. 62(September 2013): p. 138–147 DOI: 10.1016/j.ijrmms.2013.05.002.

Bibliography

6. Keating, E., Hakala, Viswanathan, H.S., Carey, R., Pawar, R.J., Guthrie, G.D. and Fessenden, J., CO2 leakage impacts on shallow groundwater: field-scale reactive-transport simulations informed by Observations at a natural analog site. Applied Geochemistry, 2013. 30: p. 136-147 DOI: 10.1016/j.apgeochem.2012.08.007.
7. Kneafsey, T., Silin, D. and Ajo-Franklin, J., Supercritical CO2 flow through a layered silica sand/calcite sand system: Experiment and modified Maximal Inscribed Spheres analysis,. International Journal of Greenhouse Gas Control, 2013. 14: p. 141-150 DOI: 10.1016/j.ijggc.2012.12.031
8. Lauchnor, E., Schultz, L., Bugni, S., Mitchell, A., Cunningham, A. and Gerlach, R., Bacterially induced calcium carbonate precipitation and strontium co-precipitation in a porous media flow system. Environmental Science & Technology Journal, 2013. 47(3): p. 1557-1564 DOI: 10.1021/es304240y.
9. Mitchell, A., Phillips, A., Schultz, L., Parks, S., Spangler, L., Cunningham, A. and Gerlach, R., Microbial CaCO3 mineral formation and stability in a simulated high pressure saline aquifer with supercritical CO2. International Journal of Greenhouse Gas Control, 2013. 15: p. 86-96 DOI: 10.1016/j.ijggc.2013.02.001.
10. Phillips, A., Gerlach, R., Lauchnor, E., Cunningham, A. and Spangler, L., Engineered applications of ureolytic biomineralization: a review Biofouling, 2013. 29(6): p. 715-733 DOI: http://dx.doi.org/10.1080/08927014.2013.796550.

Bibliography

11. Phillips, A., Lauchnor, E., Eldring, J., Esposito, R., Mitchell, A., Gerlach, R., Cunningham, A.B. and Spangler, L., Potential CO2 Leakage Reduction through Biofilm-Induced Calcium Carbonate Precipitation Environmental Science & Technology Journal, 2013. 47(1): p. 142-149 DOI: http://dx.doi.org/10.1021/es301294q.
12. Amonette, J.E., Barr, J.L., Erikson, R.L., Dobeck, L. and Shaw, J.A., Measurement of Advective Soil Gas Flux: Results of Field and Laboratory Experiments with CO2. Environmental Earth Sciences, 2012. Published online(February 17, 2013) DOI: 10.1007/s12665-013-2259-5.
13. Barnhart, E., Bowen, D., Ramsay, B., Cunningham, A.B. and Fields, M., Coal-Associated Bacterial and Archaeal Populations: Coal-Dependant Increased Bacterial Diversity. International Journal of Coal Geology, 2012. 115(2013): p. 64-70 DOI: 10.1016/j.coal.2013.03.006.
14. Bonneville, A., Dermond, J., Strickland, M., Sweeney, M., Sullivan, E.C., Heggy, E. and Normand, J., Monitoring Surface Deformation Associated with an Aquifer Storage and Recovery (ASR) Site In Pendleton, OR, as an Analog for Subsurface CO2 Sequestration. Water Resources Research, 2012. Submitted
15. Hogan, J.A., Shaw, J.A., Lawrence, R.L. and Larimer, R.L., Low-cost multi-spectral imager for detecting gas leaks indirectly from changes in vegetation reflectance. Appl. Opt., 2012. 51(4): p. A59-A66 DOI: 10.1364/AO.51.000A59

Bibliography

16. Hogan, J.A., Shaw, J.A., Lawrence, R.L., Lewicki, J.L., Dobeck, L. and Spangler, L., Detection of leaking CO2 gas with vegetation reflectances measured by a low-cost multispectral imager. IEEE J. Selected Topics Appl. Earth Obs. And Rem. Sens, 2012. 5(3): p. 699-706 DOI: 10.1109/JSTARS.2012.2202880
17. Johnson, J., Shaw, J.A., Lawrence, R.L., Nugent, P., Dobeck, L. and Spangler, L., Long-wave Infrared Imaging of Vegetation For Detecting Leaking CO2 Gas. Journal of Applied Remote Sensing 2012. 6(063612) DOI: 10.1117/1.JRS.6.063612.
18. Kihm, J., Kim, J.M., Wang, C. and Xu, T., Hydrogeochemical numerical simulation of impacts of mineralogical compositions and convective fluid flow on trapping mechanisms and efficiency of carbon dioxide injected into deep saline sandstone aquifers. Journal of Geophysical Research, 2012. 117(B06204) DOI: 10.1029/2011JB008906
19. Lageson, D.R., Larsen, M.C., Lynn, H.B. and Treadway, W.A., Applications Of Google Earth Pro to Fracture and Fault Studies of Laramide Anticlines in the Rocky Mountain Foreland Whitmeyer, S.J., Bailey, J.E., De Paor, D.G., and Ornduff, T., eds., Google Earth and Virtual Visualizations in Geoscience Education and Research, 2012. 492: p. 209-220 DOI: 10.1130/2012.2492(15)
20. Lewicki, J.L. and Hilley, G.E., Eddy covariance network design for mapping and quantification of surface CO2 leakage fluxes. International Journal of Greenhouse Gas Control, 2012. 7: p. 137-144 DOI: doi:10.1016/j.ijggc.2012.01.010.

Bibliography

21. Viswanathan, H.S., Z., D., C., L., Keating, E., Hakala, K., S., Zheng, L. and Pawar, R.J., Developing a robust geochemical and reactive transport model to evaluate possible sources of arsenic at the CO2 sequestration natural analog site in Chimayo, New Mexico. International Journal of Greenhouse Gas Control, 2012. 10: p. 199-214 DOI: 10.1016/j.ijggc.2012.06.007.
22. White, M.D., Bacon, D.H., McGrail, B.P., Watson, T.L., White, S.K. and Zhang, G., STOMP: Subsurface Transport Over Multiple Phases: STOMP-CO2 and -CO2e Guide. PNNL-21268, 2012
23. Windisch, C.F., Maupin, J.G.D. and McGrail, B.P., Soret Effect Study on High- Pressure CO2-Water Solutions Using UV-Raman Spectroscopy and a Concentric-Tube Optical Cell. Technical Report PNNL-21156, 2012
24. Windisch, C.F., Maupin, J.G.D. and McGrail, B.P., Ultraviolet (UV) Raman Spectroscopy Study of the Soret Effect in High-Pressure CO2-Water Solutions. Applied Spectroscopy, 2012. 66(7): p. 731-739 DOI: 10.1366/12-06591
25. Zhou, X.B., Lakkaraju, V.R., Apple, M., Dobeck, L., Gullickson, K.S., Shaw, J.A., Cunningham, A.B., Wielopolski, L. and Spangler, L., Experimental observation of signature changes in bulk soil electrical conductivity in response to engineered surface CO2 leakage. International Journal of Greenhouse Gas Control, 2012. 7: p. 20-29 DOI: 10.1016/j.ijggc.2011.12.006

Bibliography

26. Cunningham, A.B., Gerlach, R., Spangler, L., Mitchell, A., Parks, S. and Phillips, A., Reducing the risk of well bore leakage of CO2 using engineered biomineralization barriers. Energy Procedia, 2011. 4: p. 5178-5185 DOI: 10.1016/j.egypro.2011.02.495.
27. Pruess, K., Integrated Modeling of CO2 Storage and Leakage Scenarios Including Transitions between Super- and Sub-Critical Conditions, and Phase Change between Liquid and Gaseous CO2. Greenhouse Gases: Science and Technology, 2011. 1(3): p. 237-247 DOI: 10.1002/ghg.024.
28. Xu, T., Spycher, N., Sonnenthal, N., Zhang, G., Zheng, L. and Pruess, K., TOUGHREACT Version 2.0: A Simulator for Subsurface Reactive Transport under Non-isothermal Multiphase Flow Conditions,. Computers & Geosciences, 2011. 37(6): p. 763-774 DOI: 10.1016/j.cageo.2010.10.007.
29. Xu, T., Zheng, L. and Tian, H., Reactive Transport Modeling for CO2 Geological Sequestration. Petroleum and Science and Engineering, 2011. 78(3-4): p. 765-777 DOI: 10.1016/j.petrol.2011.09.005
30. Zhang, W., Xu, T. and Li, Y., Modeling of fate and transport of coinjection of H2S with CO2 in deep saline formations. Journal of Geophysical Research-Solid Earth, 2011. 116(B02202): p. 13 DOI: 10.1029/2010JB007652.

Bibliography

31. Keating, E., Hakala, J.A., Viswanathan, H.S., Capo, R., Stewart, B., Gardiner, J., Guthrie, G.D., Casey, J.W. and Fessenden, J., The challenge of predicting groundwater quality impacts in a CO2 leakage scenario: Results from field, laboratory, and modeling studies at a natural analog site in New Mexico, U.S.A. Energy Procedia, 2010. 4: p. 3239-3245 DOI: 10.1016/j.egypro.2011.02.242.
32. Krupa, K.M., Cantrell, K.J. and McGrail, B.P., Thermodynamic Data for Geochemical Modeling of Carbonate Reactions Associated with CO2 Sequestration –Literature Review. PNNL-19766, 2010
33. Silin, D., Tomutsa, L., Benson, S.M. and Patzek, T., Microtomography and Pore Scale Modeling of Two-Phase Fluid Distribution. Transport in Porous Media, 2010: p. 1-21 DOI: 10.1007/s11242-010-9636-2.

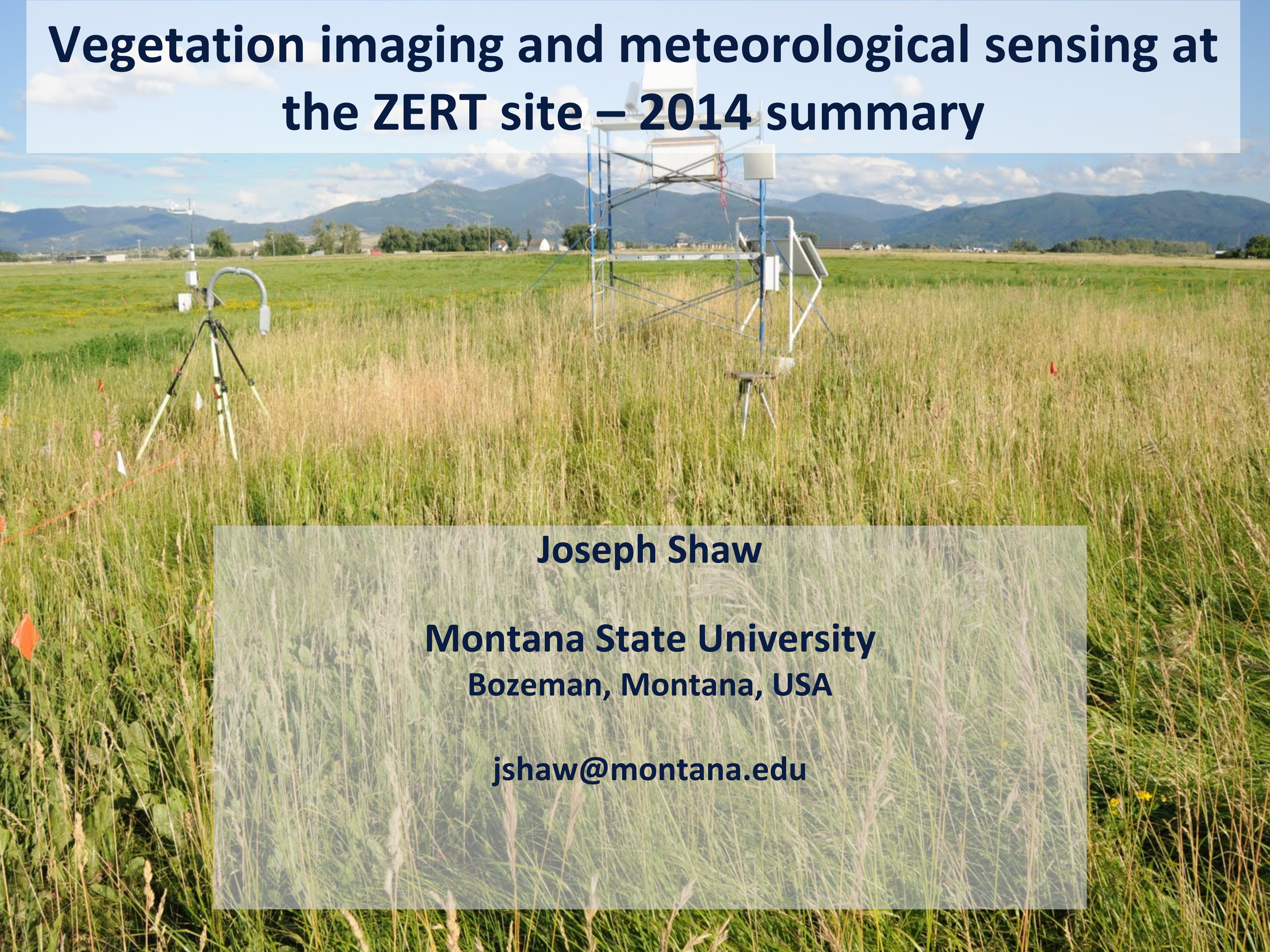

Vegetation imaging and meteorological sensing at the ZERT site – 2014 summary

Joseph Shaw

Montana State University
Bozeman, Montana, USA

jshaw@montana.edu

Vegetation imaging test at ZERT field

Principle: detect leaking gas from induced plant stress

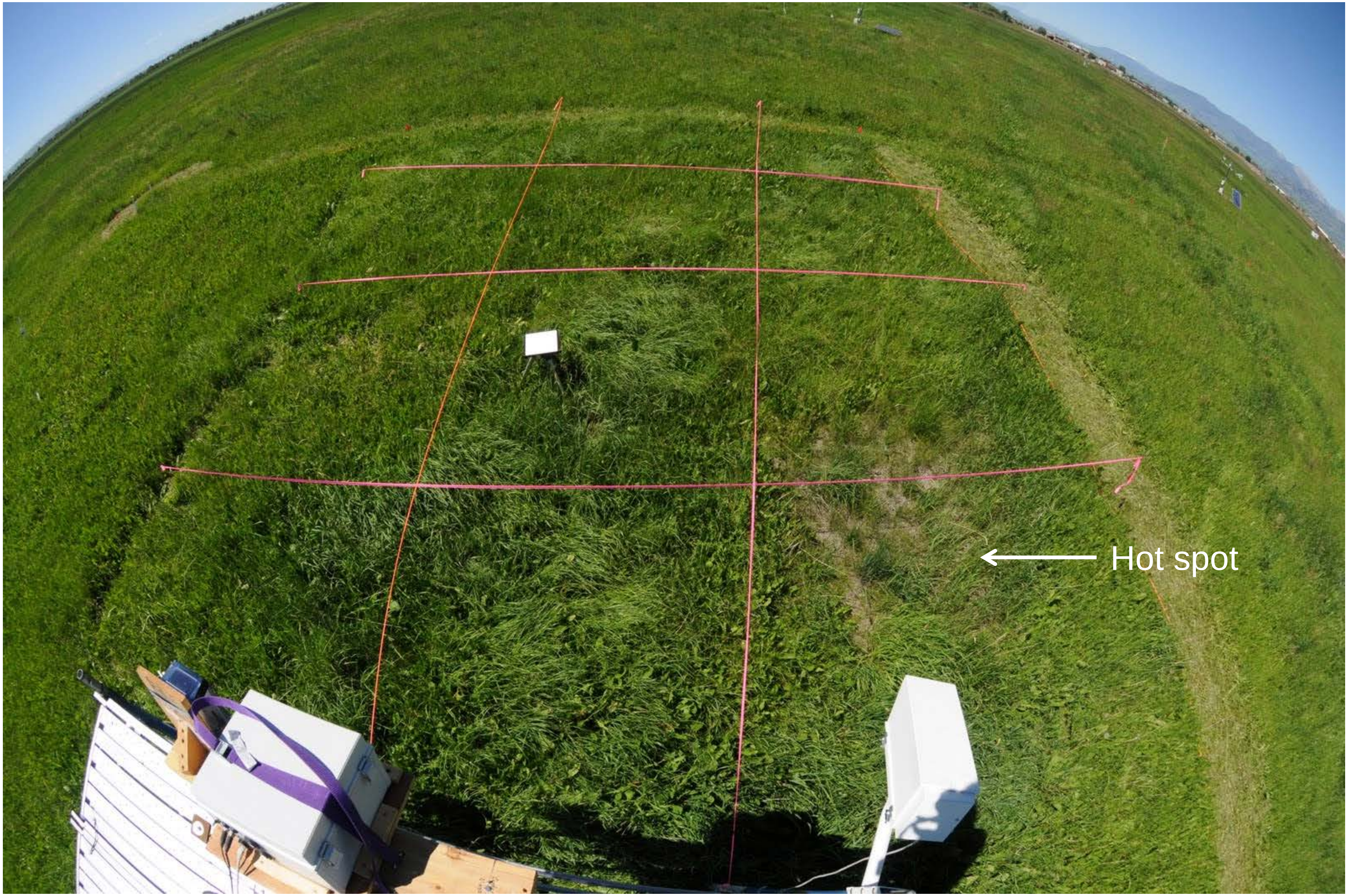

Visible & NIR imaging to locate CO2 leak via plant stress

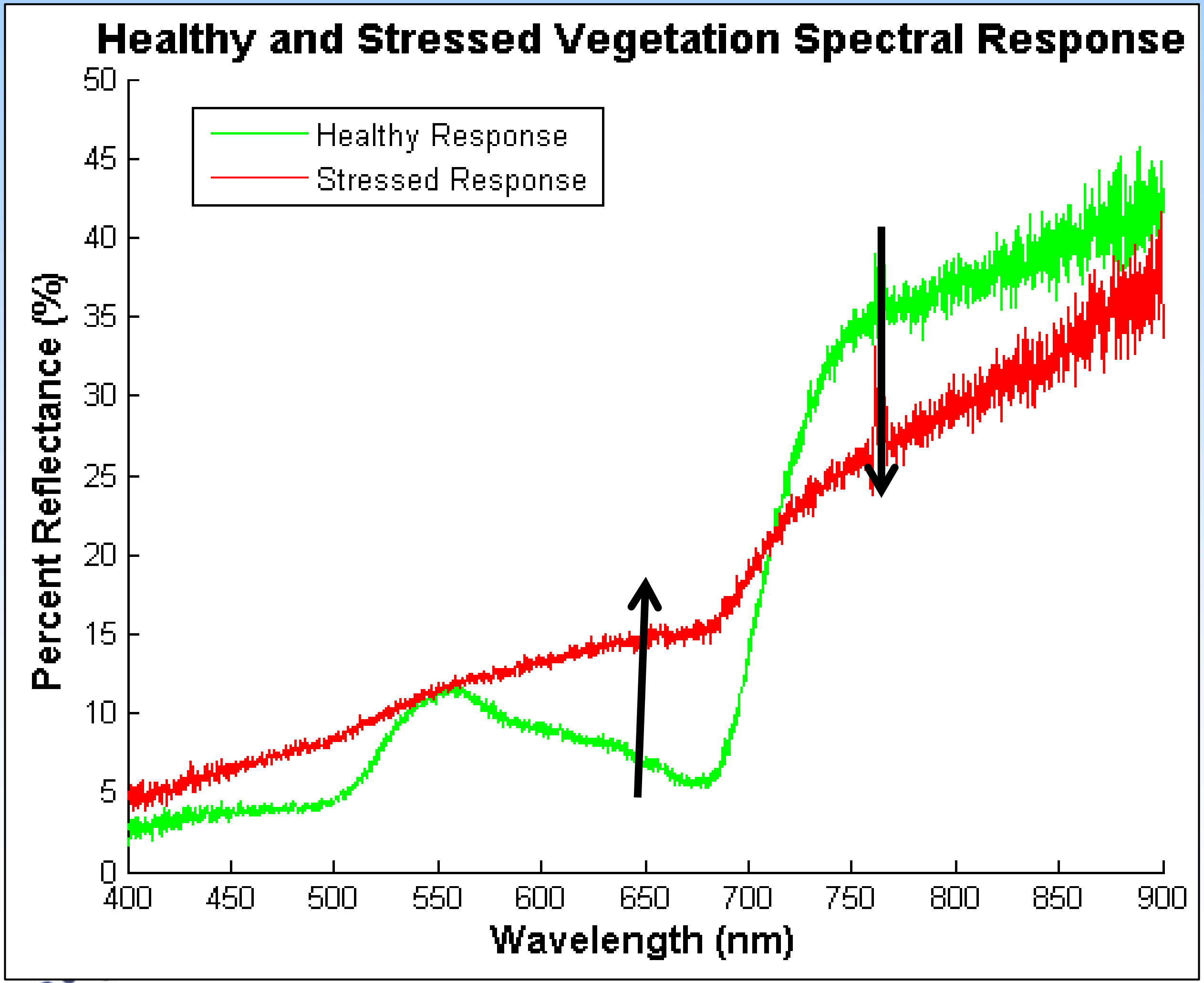

Normalized Difference Vegetation Index

$$NDVI = \frac{\rho_{NIR} - \rho_{RED}}{\rho_{NIR} + \rho_{RED}}$$

ZERT Zero Emissions Research and Technology

MONTANA STATE UNIVERSITY

Tethered balloon multispectral imaging

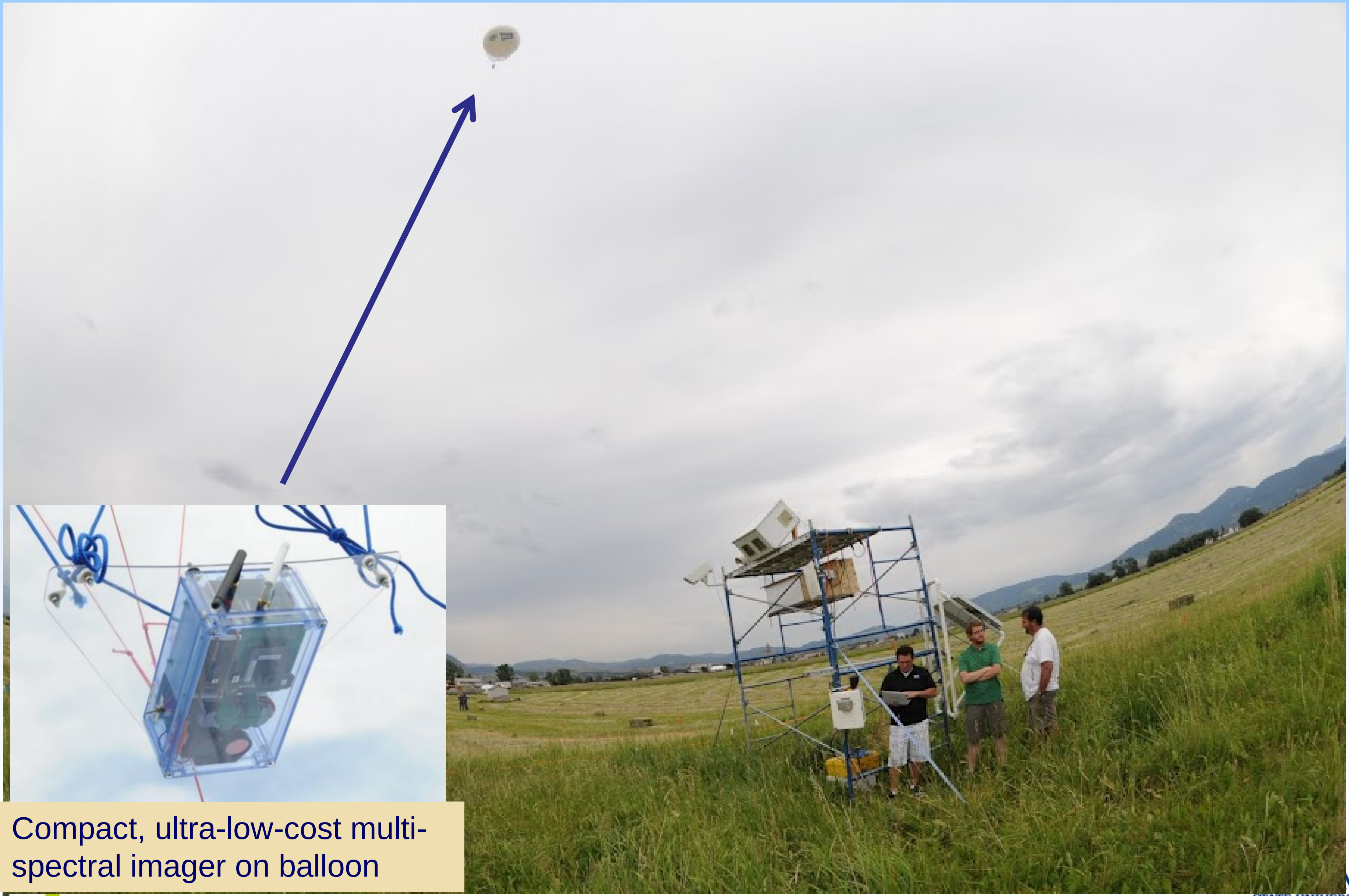

Compact, ultra-low-cost multi-spectral imager on balloon

NDVI measured with balloon camera & scaffold camera

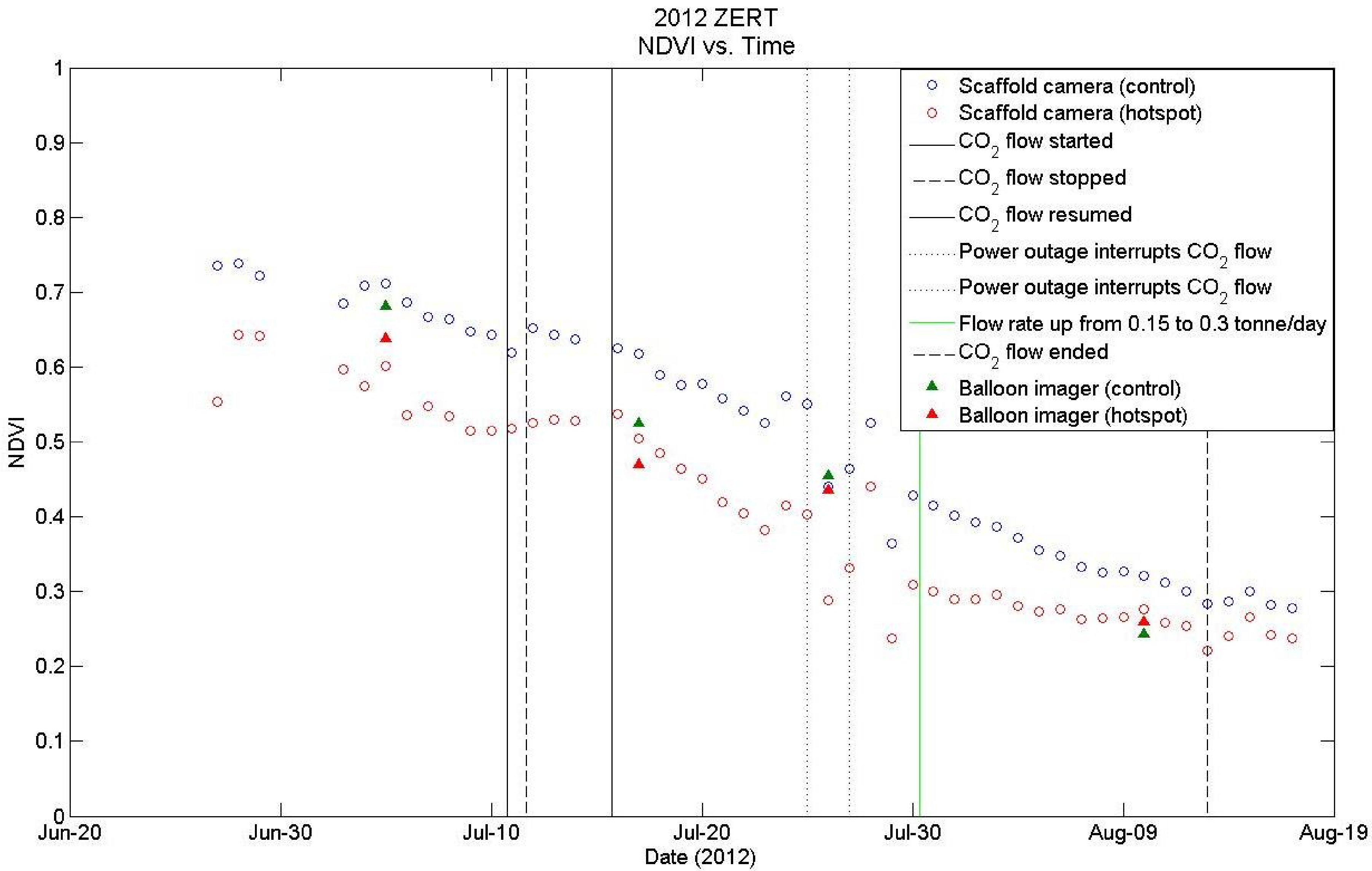

Thermal imaging also detects leaking gas

10 μm IR images before & after CO_2-induced plant stress

Before | After

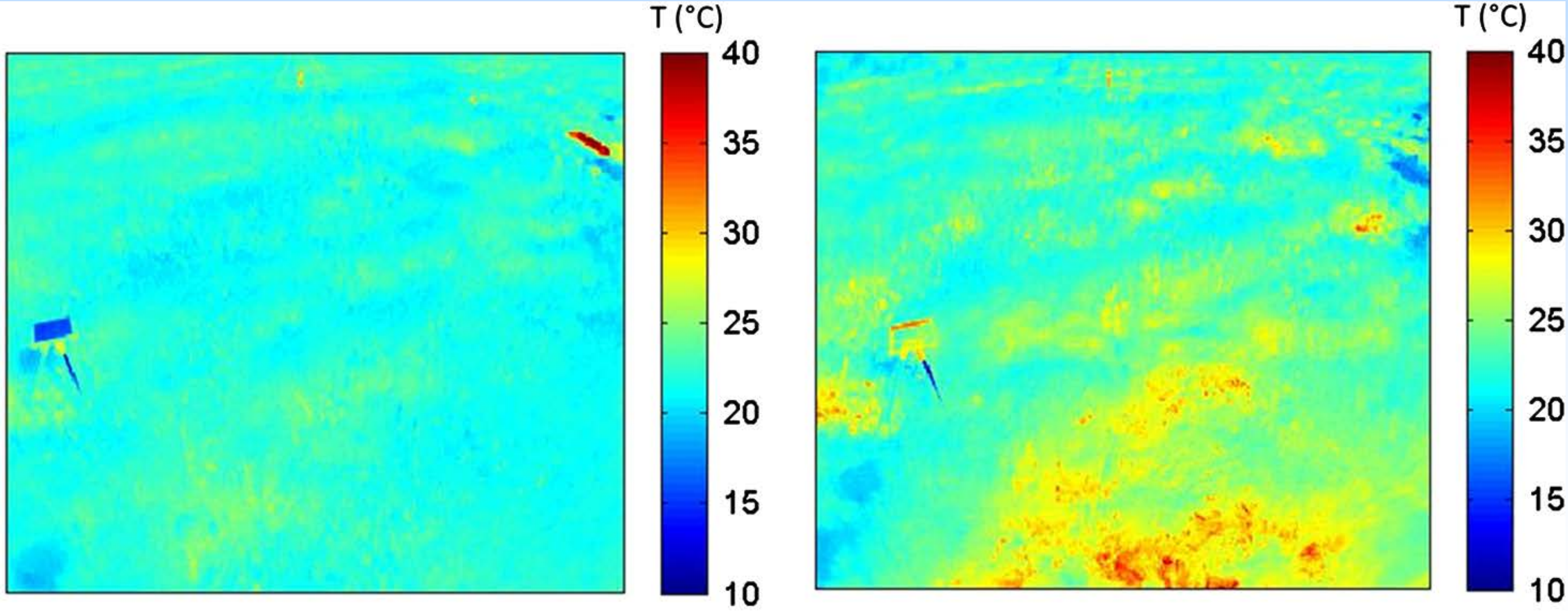

ZERT Zero Emissions Research and Technology

MONTANA STATE UNIVERSITY

Hot spot emits higher IR radiation after start of CO_2 flow

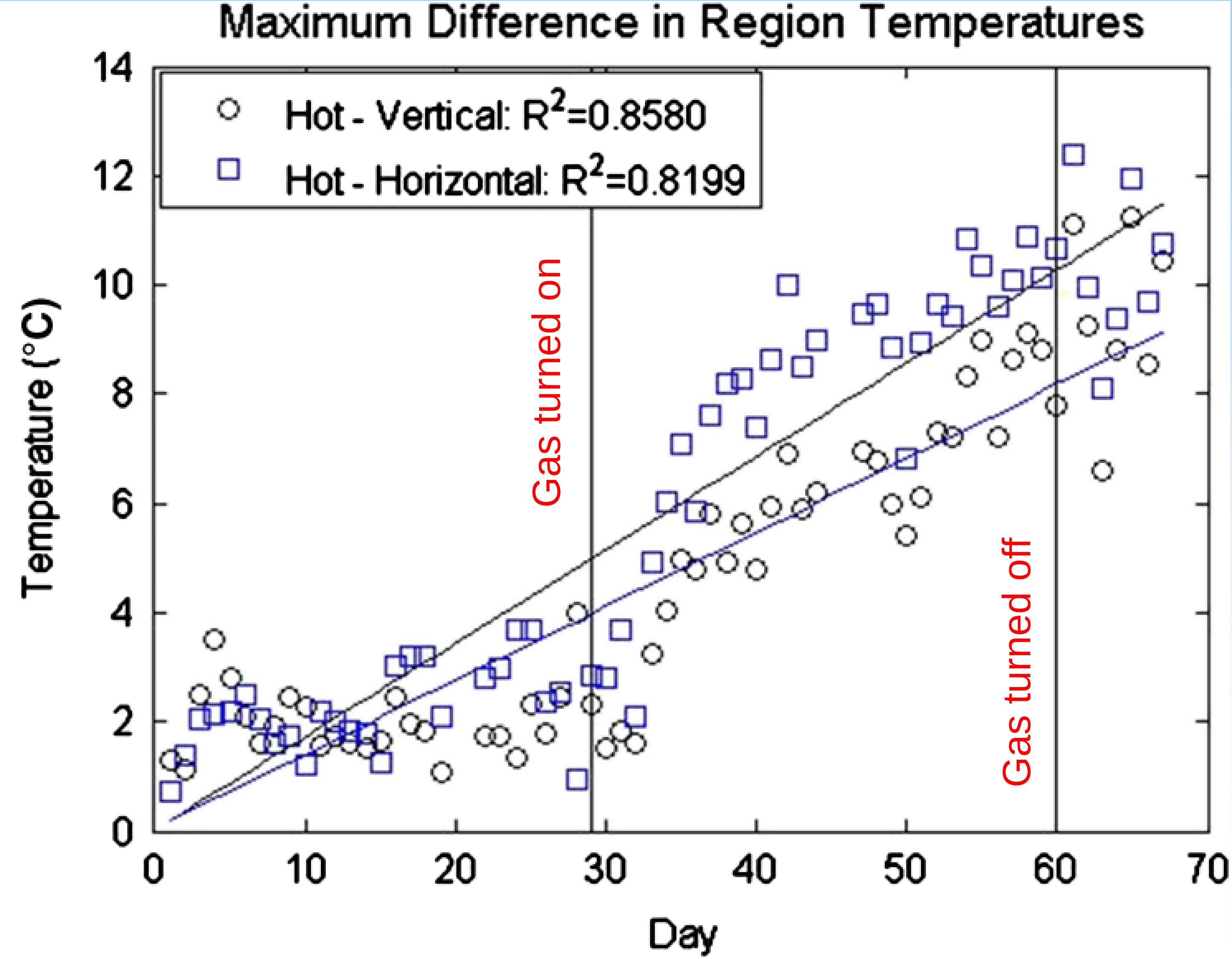

ZERT weather station study

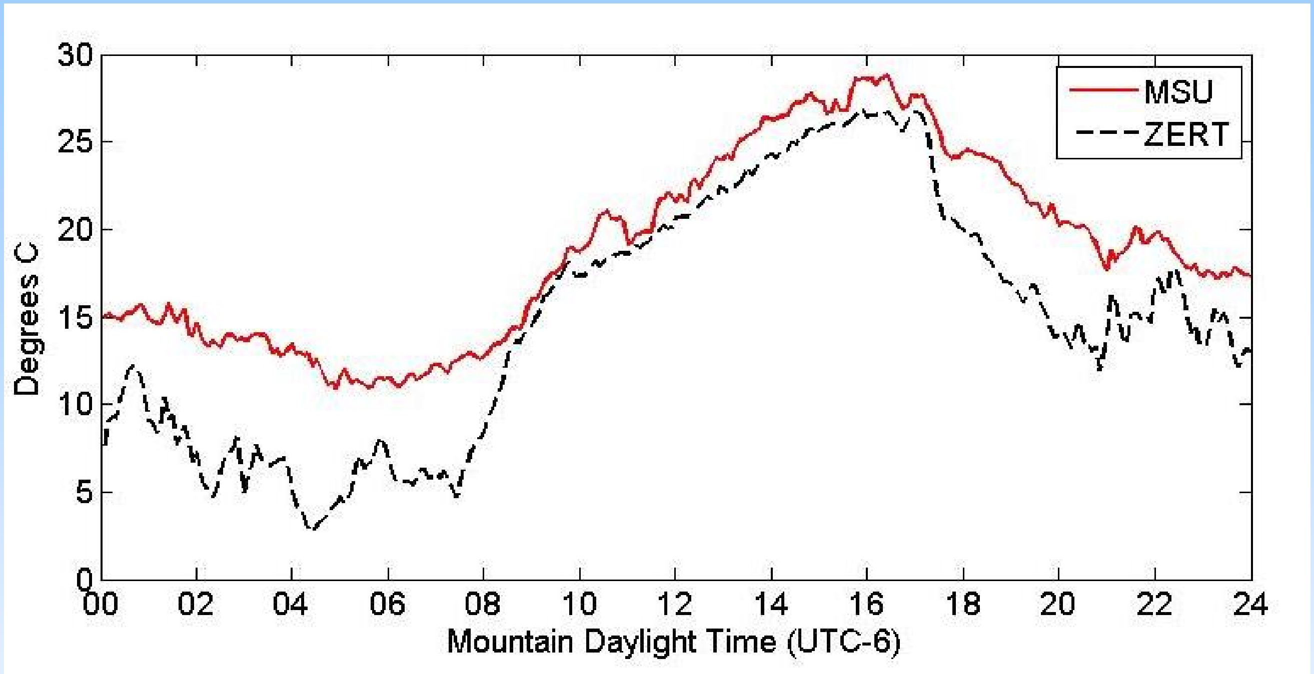

Two identical sensors at ZERT and MSU

3rd identical sensor mounted on backpack

- Confirmed calibration of each weather station
- Temperature variation map indicates existence of campus heat island

MSU - mobile

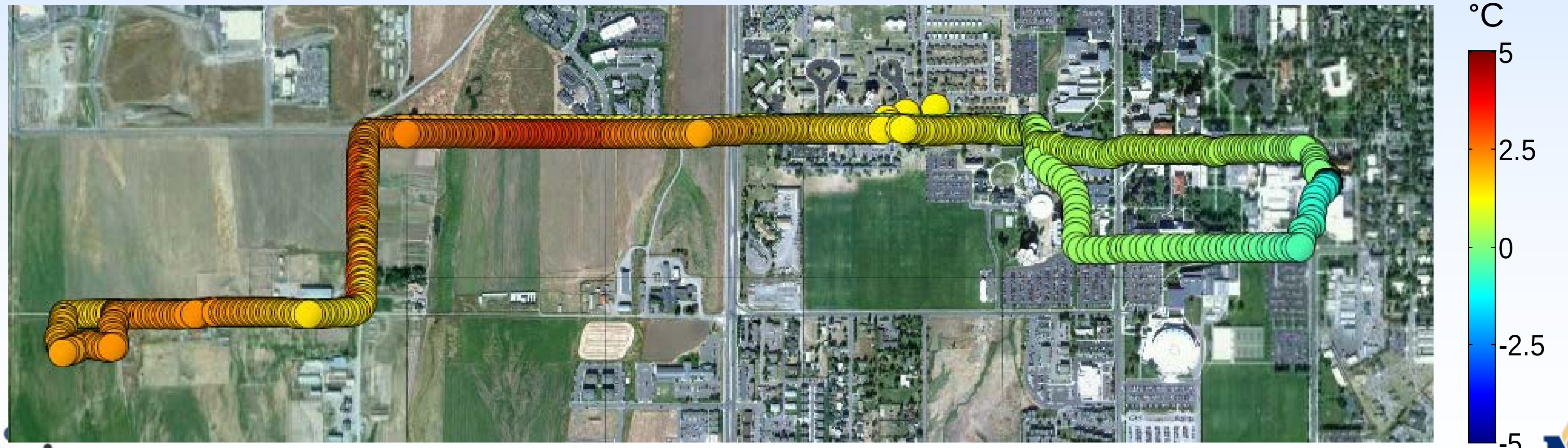

Zero Emissions Research and Technology

MONTANA STATE UNIVERSITY

Heat island also varies throughout town

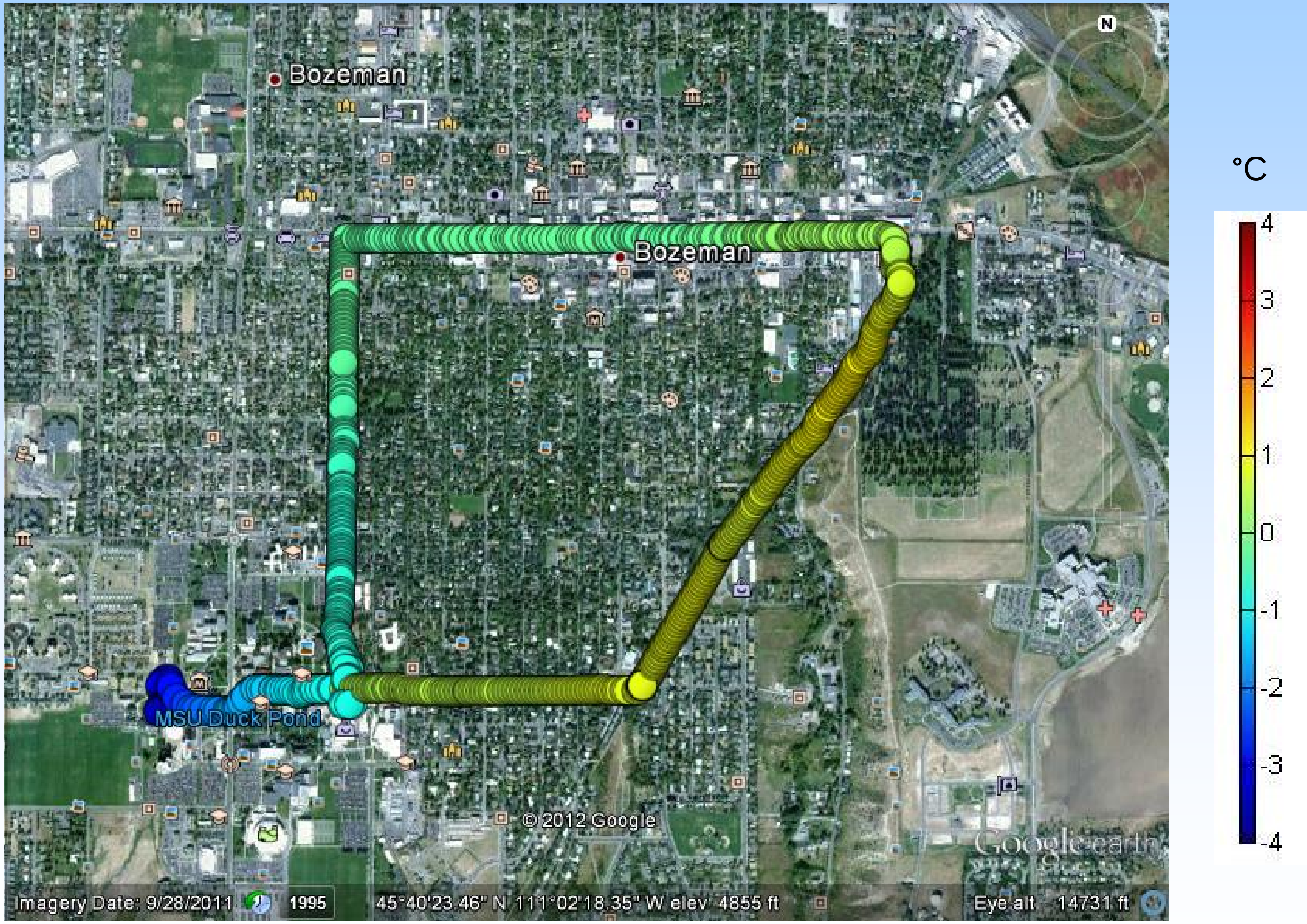

Thermal camera used to understand heat island

Two sample regions: grass and concrete

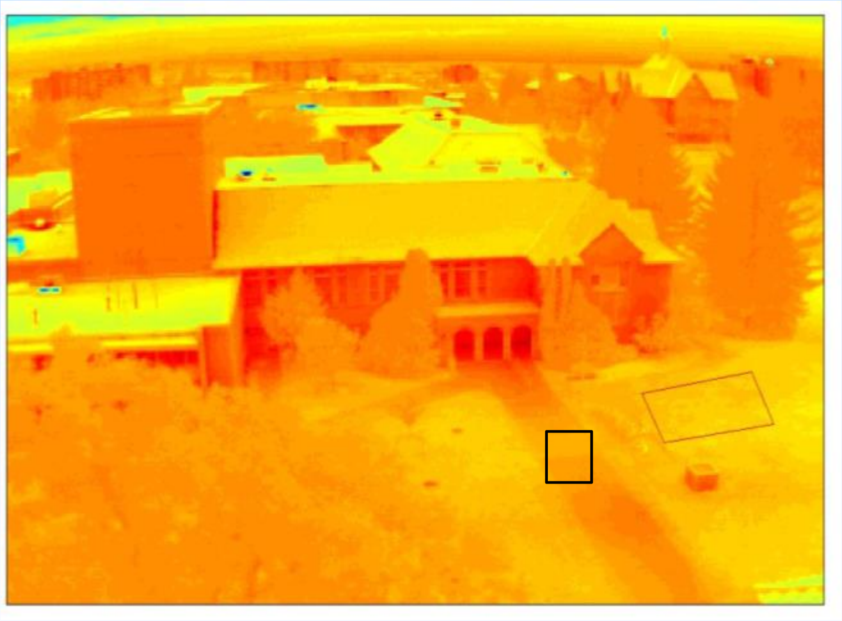

Zero Emissions Research and Technology

MONTANA STATE UNIVERSITY

Higher IR radiation from concrete warms the air

IR temperatures and air temp

Sidewalk is warmer except with direct Sun

Clouds explain wiggles in daytime IR temps

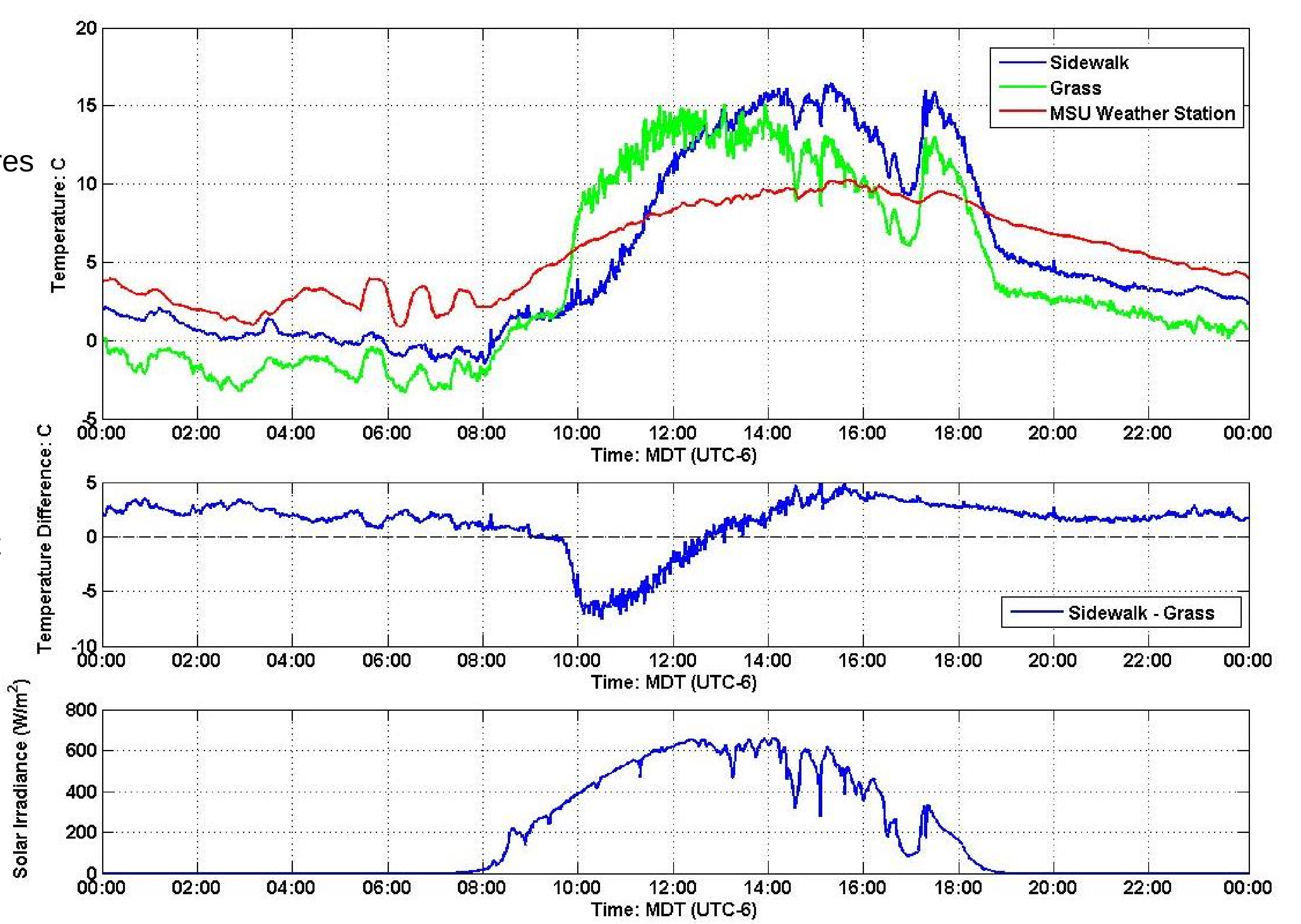

Higher IR radiation from concrete warms the air (2)

IR & air temps

Sidewalk is warmer except in direct Sun

Clouds explain wiggles in daytime IR temps

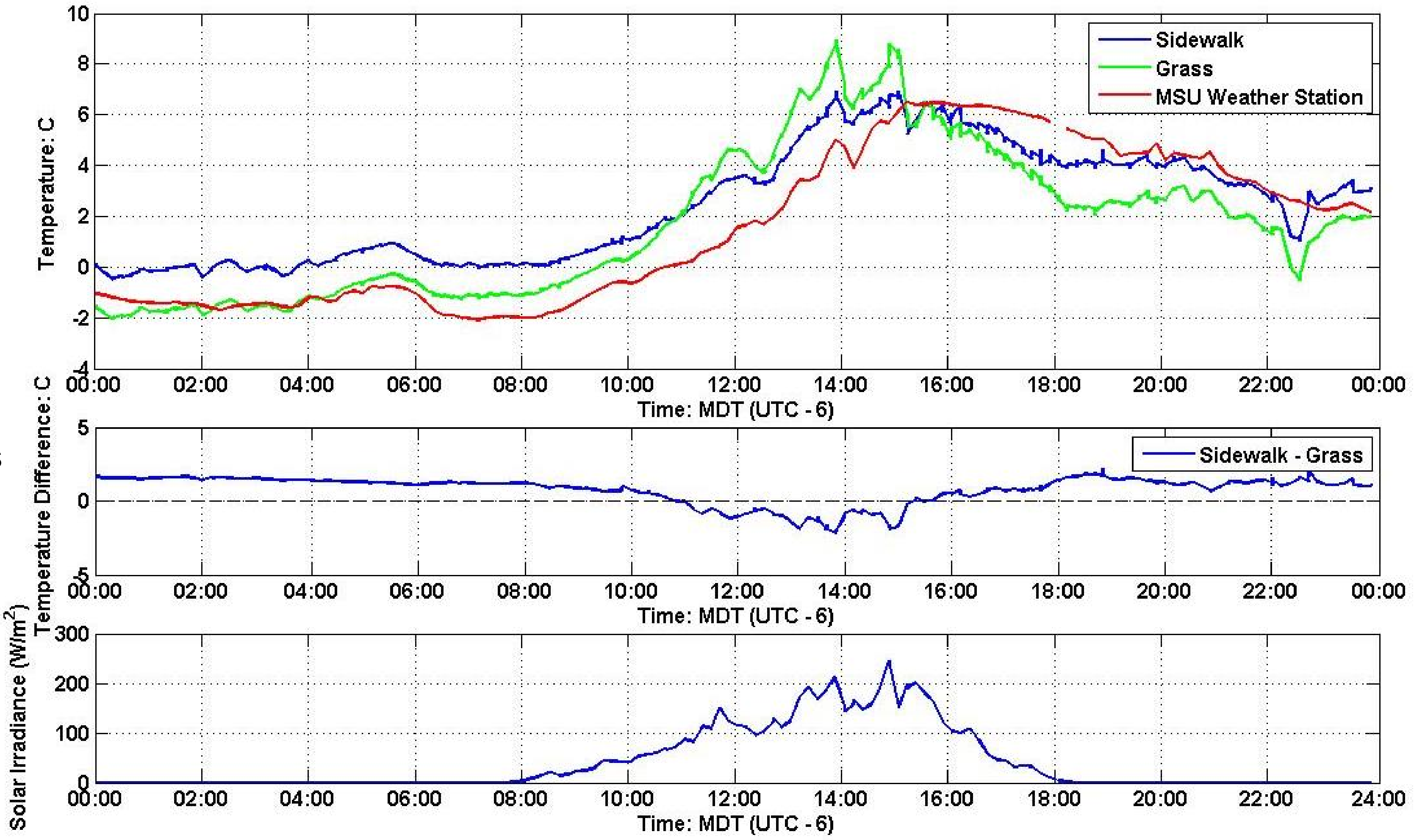

Summary

- Leaking CO_2 gas has been detected via plant stress with visible and NIR imaging and with thermal IR imaging;

- Balloon-borne vis-NIR camera gives same results, but over much larger area and without airplane;

- ZERT weather station is accurate, but difference from MSU station helped us understand heat islands…